Chapter 2. Reactor Pressure Vessel Design

J. Föhl
Staatliche Materialprüfungsanstalt (MPA)
Universität Stuttgart, Germany

1 Introduction

The design of the RPV has to take into account all functional requirements to provide hot water (pressurized water reactor, PWR) or steam (boiling water reactor, BWR) and all possible deviations from normal operating conditions as well as loads resulting from low probability external events such as earthquake and air plane crash.

With regard to neutron irradiation the discussion of RPV design is limited to the core belt line of the vessel, which is defined as the region where the material accumulates a fluence of more than 10^{21} m^{-2} (E > 1 MeV) [1, 2]. However, all loading patterns resulting from normal operation, emergency and upset conditions in the plant have to be considered in their effect on the RPV.

The design process includes a variety of different tasks. Starting with the specification of the functional parameters the main areas are:

- specification of initial material properties with sufficient reserve accounting for time depending degradation.

- reliable determination of material properties and the pressure and state of flaws in the component (quality assurance)

- determination of loading (operating, service) conditions

- time dependent degradation under service conditions

- surveillance of material and flaw state as well as monitoring of service conditions

- assumptions for worst case conditons with respect to loading spectrum, material and flaw state.

For the assessment of overall safety, validated computer codes (thermal hydraulics and finite element codes) and fracture mechanics concepts must be available to determine

- pressure and temperature as a function of time for all possible and postulated events in the plant, considering the plant specific interaction of components and events

- loading (stress, strain) of the component for a given pressure and temperature under steady state and transient conditions

- stress intensity and strain distribution of the component assuming the presence of flaws.

Failure of the reactor pressure vessel can be by leakage or by bursting, however, both cases have to be prevented by adequate design according to the Code requirements for boiler and pressure vessels as it is e.g. the ASME Code in the US or the KTA-Code in Germany. Crack initiation may occur, but arrest of the crack has to be assured at a depth of 75% of the wall thickness [3].

The likelyhood of the occurrence of an event is assumed and can be estimated on a probabilistic basis. In consequence of an event two different safety strategies are in current use. In the probabilistic safety approach the vessel is assumed to fail under some severe events which, however, have an extremely low probability. Alternatively, the deterministic safety approach determines design conditions under which catastrophic failure is ruled out even in case of the most severe events. The philosophy of the deterministic approach is based on a material toughness concept with additional independent redundancies as outlined in the German "Basis Safety Concept", Fig. 1, [4]. The redundant measures are:

- "multiple parties testing" to assure and record the initial quality of the component

- understanding of the thermo-mechanical behavior of the material and thus to establish the "worst case" material state

- continuous monitoring of safety-relevant "in-service parameters" to assure that the design assumptions cover all events conservatively

- availability of validated computer codes, fracture mechanics concepts and non destructive examination (NDE) and evaluation methods.

The substential prerequisite, however, for a "basis safe design" is the production of an ingot with optimized chemical composition regarding alloying, accompanying and trace elements including a reduced segregation pattern. This incorporates low sensitivity against degradation during manufactoring (forging, heat-treatment, welding, post weld heat-treatment), provides high initial toughness and assures a minimum of defects. Additionally the sensitivity against ageing under service conditions is improved.

With respect to the weld, improvements have been made by adequate selection of flux in combination with requirements on the chemical composition of the weld wire, welding parameters such as weld bead size and sequence to minimize the coarse grained areas in the heat affected zone (HAZ) [5].

2 Service Conditions

For the core belt line region of the reactor pressure vessel, the safety relevant parameters are:

- pressure
- temperature
- neutron irradiation and
- coolant.

Materials used for the RPV are fine grained high strength ferritic steels which are protected against corrosion with an austenitic steel cladding. The operating temperature is commonly about 280 to 290°C, the operating pressure is at 7 MPa for BWR and up to 15 MPa for PWR.

Heavy components are susceptible to potential crack formation during fabrication, particularly resulting from welding and cladding with subsequent stress relief heat treatment. Because some cracks may remain undiscovered by non destructive examination (NDE), fracture mechanics analyses to evaluate their significance are required. In the safety assessment flaw sizes are postulated covering realistic and worst case conditions. The assumptions include subsurface cracks and surface cracks penetrating the cladding.

The degradation of the RPV material is essentially determined by the accummulated neutron fluence, therefore, efforts were undertaken to reduce the neutron flux at the vessel wall. This could be achieved by increasing the distance between the core edge and the vessel wall.

Neutron exposure is defined differently, in different countries. Some consider only neutrons with energies of $E > 1$ MeV, others set the threshold at a lower level e.g. 0.5 or 0.1 MeV. Reactors built in the 1960s were of smaller dimensions and the design life fluence (DLF) for forty years (load factor 80%) was in the order of 4 to $5 \cdot 10^{23}$ m^{-2} ($E > 1$ MeV), which is not in accordance with todays reduced DLF requirements e.g. in Germany of $1 \cdot 10^{23}$ m^{-2} ($E > 1$ MeV) [3]. Therefore the neutron flux at the vessel wall of those reactors was drastically reduced by means of a changed core loading and shielding elements inserted additionally (see section 2.7.1).

Since it is known that welds incorporate a high potential for material degradation, the number of welds in the RPV was reduced for the advanced reactor design so that seamless forged shells were used rather than plates with axial weld seams.

In the last 25 years the design power of generating units has increased up to 1300 MW (electric) and these require larger RPVs. In particular the shells in the core region were made as large as possible to further minimize the number of welds and increase the water gap between the core and the pressure vessel wall. With the large inner diameter of up to 5000 mm the wall thickness increased to 250 mm, Fig. 2. Producing such heavy ingots and fabricating large vessels of high quality was a big challenge to the industry. Examples of vessel dimensions are shown in Fig. 3.

For the large units (advanced design) the design life fluence is much lower and amounts to about $5 \cdot 10^{22}$ m^{-2} for PWRs and $5 \cdot 10^{21}$ m^{-2} (E > 1 MeV) for BWRs, respectively. In Germany for example the licensing requirement is not to exceed a fluence of $1 \cdot 10^{23}$ m^{-2} (E > 1 MeV) in 32 effective full power years [3] which forced the industry to produce larger vessels than elsewhere. A comparison of water gaps for some typical reactors is shown in Fig. 4. This difference in design becomes obvious by comparing the two 1300 MW plants which represent the German and the US design [6].

Besides the geometrical parameters the neutron flux is determined by the core loading scheme, which is different in BWRs and PWRs and is the reason for the generally low flux in BWRs. Modifications in the fuel element arrangement were also made to reduce the design life fluence for older PWR reactor pressure vessels.

3 Design Criteria

The major criteria on which the design is based with respect to neutron irradiation are:

- pressure/temperature-time relationships and the resulting mechanical and thermal stresses including residual stresses from fabrication (load paths)

- quantitative data on change of material properties due to ageing effects, essentially by neutron irradiation

- miniumum material properties requirements which allow safe operation or at least safe shut down in case of emergency and accident conditions.

This is shown in Fig. 5 [7]. Each of the tasks mentioned above was and is still subject of intense research and development (R&D) work. Progress has been made in the determination of the effect of neutron irradiation on materials the knowledge of which can generally be applied in the safety assessment. However, the exploration of the most critical loading path has to be performed for each individual plant.

Great efforts have been made to assess the limit for material properties at which catastrophic failure of a component can be excluded. Investigations in this direction were enhanced because several older reactors will reach their end-of-life (which can be defind in various ways) within the next decade. In this connection, decisions about life extension may have to be made. Furthermore, the weld of some US-reactors had low toughness already at the beginning of life while others have been susceptible to neutron irradiation [8], so the toughness values come close to the limits set by the relevant Codes.

4 Design Concepts

The safety assessment concentrates primarily on the prevention of brittle failure. Therefore the conditions must be defined under which brittle failure can be excluded. This is the case when the loading of the component occurs in a regime sufficiently above the Nil Ductility Transition Temperature T_{NDT} [9] which is conservatively determined from both the Charpy and the drop-weight test. The reference temperature RT_{NDT} is the highest temperature comparing T_{NDT} with T_{68J} - 33 K and $T_{0.9\ mm}$ - 33 K, respectively. T_{68J} (temperature at which 68 J is reached) and $T_{0.9\ mm}$ (temperature at which 0.9 mm lateral expansion is reached) are derived from Charpy specimens testing with at least 3 specimens or from an energy/temperature and lateral expansion/temperature curve [10, 11].

4.1 Transition Temperature Concept

On the basis of the RT_{NDT} a temperature/pressure limit-curve (modified Porse diagram) can be established which separates the regime in which a component can be operated safely, from a so called "not allowed" ("prohibited") regime in which brittle failure has to be considered, Fig. 6. This concept is based upon the failure assessment diagram as introduced by Pellini [9]. It is concluded that even for large flaws brittle failure of the component will not occur at a high enough temperature above T_{NDT}. A basic assumption in this concept is that only primary stresses are acting arising from internal pressure.

The main concern of in-service material degradation is the increase in transition temperature and drop in upper shelf toughness. The degree of material degradation is usually determined with Charpy specimens only, measuring the shift of the transition temperature at an energy level of 41 J (ΔT_{41J}) and the drop in upper shelf energy (ΔUSE) [1, 2, 12, 13]. The energy level of the shift criteria has changed in the past from 68 J to 41 J, because the 41 J level is more closely related to NDT. However, in addition to that criterion, for some materials the upper shelf energy has dropped to a level close to 68 J, so that a shift determined at that level would be unrealistically high and in some cases the shift could not be determined at all. In some countries the shift is determined at other energy levels than 41 J, e.g. 49 J as in the ex-USSR.

To account for material degradation in the safety analysis, the Porse diagram has to be a d j u s t e d by shifting the curve to a higher temperature for that amount which can be derived from the shift of the transition temperature as determined from the Charpy energy-temperature curve at an energy level of 41 J,

$$RT_{NDT} \text{ (adjusted)} = RT_{NDT} + \Delta T_{41J}. \qquad (1)$$

An example for an adjusted pressure/temperature limit curve is also shown in Fig. 6.

As a preventive measure for RPVs with high shift in transition temperature, an automatic locking system has been introduced in some reactors to assure that no combination of pressure and temperature can occur in the prohibited regime.

4.2 Fracture mechanics concept

The transition temperature approach does not allow the quantification of the safety margin in flawed structures and cannot take into account secondary stresses. For this and other reasons the fracture mechanics approach was introduced. This compares the fracture toughness of the material with the stress intensity in a component, Fig. 7. According to some national Codes [14, 3] this approach is only applied where the linear elastic fracture mechanics regime (LEFM) is valid.

The prerequisites for using this approach are:

- reliable fracture toughness data of the material with regard to its transferability to large structures and complex geometries

- knowledge or reliable assumptions about flaw state in the component

- appropriate codes to compute the stress intensity for complex loading situations and geometries.

4.2.1 Crack initiation

For the design consideration the reference fracture toughness curve is used and fixed by the Reference Temperature RT_{NDT} as defined in section 4 above. The adjustment necessary to account for the material degradation is also made according to the transition temperature shift at the 41 J level.

From fracture mechanics testing of RPV steels a K_{IR}-curve was established as a lower bound curve that has to be used in the design phase [3, 14]. However, if actual and reliable fracture toughness data of the component are available, then these data may be used instead.

The load path has to be calculated for normal operating, emergency and faulted conditions. The size of the crack to be assumed in the safety assessment is either a semi-elliptical surface flaw with the depth a = 1/4 T and b = 1.5 T (where T = wall thickness) or an infinitely long flaw with a depth depending on the reliability of NDE techniques multiplied by a factor of two to cover uncertainties.

The 1/4 T flaw is the basis for normal operating conditions for which the stress intensity is to be calculated with a safety margin of a factor of two for the primary stresses as shown in equation (2):

$$K_I = 2\ K_I(p) + K_I(th) \qquad (2)$$

$K_I(p)$ stress intensity resulting from internal pressure

$K_I(th)$ stress intensity resulting from thermal stresses

The assumption of an infinitely long flaw is used for the calculation of the behaviour under severe transients, because the extension of shallow cracks along the surface - to grow to a long crack - occurs before the crack penetrates the wall in the thickness direction [15]. In the case of emergency and faulted conditions the stress intensity can be calculated according to

$$K_I = K_I(p) + K_I(th) + \text{others} \qquad (3)$$

The primary stresses do not have to be multiplied by a factor of two as required for normal operating conditions, however, the theoretical crack depth assumption has to be twice the size certified by non destructive examination.

A typical load path for start-up and shut-down is shown in Fig. 7. The comparison of the load path with the fracture toughness curve shows clearly that the safety margin has to be considered in two directions, one refers to load, the other to temperature. Failure of the component cannot be excluded when the load path intersects the fracture toughness curve (exceptions are discussed in section 4.2.3).

On the fracture mechanics basis the effect of transient loading on cracks can be assessed. The loading path for the most severe transient has to be evaluated for each individual plant. One critical accident assumption is the rupture of a small pipe (small break loss of coolant accident, LOCA) or a leak of corresponding size. In that case, the emergency core cooling pumps come into action feeding cold water into the vessel while the pressure is essentially maintained at saturation pressure or drops very slowly. As a consequence the inner surface of the RPV wall cools down rather rapidly building up thermal stresses which are in addition to the stresses resulting from internal pressure [16, 17, 18].

For a postulated leak of 1960 mm² (I.D. = 50 mm) and a coolant temperature of 30°C the pressure-time and temperature-time path responsible for the load on the pressure vessel is shown in Fig. 8. In this example a slight repressurization occurs after about 10 min. The resulting stress intensity was computed for different crack sizes (crack depth a) and is plotted in Fig. 9 for a circumferential flaw and in Fig. 10 for an axial flaw.

The higher primary stress for the axially oriented flaw leads consequently to high stress intensity values. Because the stress intensity was computed using linear elastic methods, unrealistically high values are reached shortly after start of cool down in a temperature range where ductile behavior of the material can be expected. The linear elastic fracture mechanics approach does not take into account any ductile (stable) crack extension. In the safety assessment, the upper temperature regime is only covered by results of Charpy impact test and associated experience. In this respect, failure of the component can be excluded when the Charpy upper shelf toughness is not lower than 68J. The calculation of the stress intensity for a circumferential crack with respect to brittle crack initiation, shows that small flaws are even more dangerous than large ones [19]. In the case of ductile (stable) crack extension, however, large flaws are controlling the process.

For emergency core cooling (ECC) events the K_{Ic}-curve (static crack initiation) may be used instead of the K_{IR}-curve. The fracture toughness of materials with high sensitivity against neutron irradiation has to be adjusted at high temperatures, according to RT_{NDT} (adjusted). In that case the slope of the K_{Ic}-curve and the reliable calculation of the load path are of great importance with respect to possible intersection with the load path and thus to the lifetime for which safe operation can be assured.

4.2.2 Crack arrest

Since during ECC a temperature gradient through the wall exists, which depends strongly on the time after cool down has begun, Fig. 11a the secondary stresses are dominant in building up the stress intensity with a gradient across the wall , Fig. 11b. In case of brittle crack initiation during ECC the crack will grow rapidly into a field of higher temperature.

Once the crack tip has jumped to a location at which the material is in the upper shelf toughness regime the crack could arrest although the stress intensity may have increased during this crack extension. In general the stress intensity first increases with time and decreases after a certain time, Fig. 11c, however, as the material temperature at the new crack tip decreases and the stress intensity is still high enough a second crack initiation may occur. For the entire ECC path the correlation between temperature, crack depth, stress intensity and time can be computed. On this basis two curves

$$K_I = K_{Ic} \quad \text{and} \quad K_I = K_{Ia}$$

can be established as shown schematically in Fig. 12 from which the sequence of crack initiation and arrest can be evaluated [18, 19].

According to some national Codes [3, 20], crack initiation may be considered, when crack arrest can be assured at less than 75% of the wall thickness. If this approach is being applied it becomes obvious that reliable initiation and arrest toughness data require to be guaranteed.

4.2.3 Warm prestressing effect

The warm prestressing effect was discussed as long ago as the early 1970s [21]. It refers to the fact that under conditions of decreasing stress intensity with time a crack cannot initiate. This situation occurs during ECC as shown in Fig. 9 and 10, respectively. There it is supposed that at the time when the load path intersects the K_{Ic}-curve with a negative slope - indicating decrease in K_I with time - a crack never will initiate. Previously it was only thought that overstressing of a sharp crack in the ductile regime would blunt the crack tip and thus crack initiation at lower K_I values would be rendered more difficult. Further considerations of the mechanism of brittle crack initiation made clear that the warm prestressing effect can be explained on the basis of the mobility of dislocations [22].

When a certain K_I value is applied to a structure in the ductile regime a plastic zone is being formed at the crack tip depending on the stress state and the deformability of the material under the given constraint (see Chapter 5). During cool down of the material at constant stress intensity (path 1) no additional energy has to be stored in the material and thus there is no driving force to move dislocations. Although the load path (horizontal curve) intersects the K_{Ic}curve, Fig. 13, crack initiation cannot occur. This is even more so in the case of decreasing K_I (path 2).

For this reason a limit can be established beyond which crack initiation is not possible. This is the point when the maximum stress intensity has been reached. However, attention has to be drawn to the particular case of repressurization. If, after the intersection of the load path due to repressurization the stress intensity increases, crack initiation has to be expected. For highly embrittled materials and severe load paths the warm prestressing effect is an essential item in the safety analysis. Several studies have been carried out to demonstrate the warm prestressing effect [23]. The benefit, however, is restricted to load cases for which repressurization can reliably be excluded.

5 Design curves to account for material in-service degradation

From fracture mechanics analyses it became obvious that knowledge about the fracture toughness/temperature curve was essential. In the unirradiated condition the lower limit curve for crack initiation has been well established for reactor pressure vessel steels used in the "western" countries [11, 14] as a conservative lower bound. In addition to that the procedure of RT_{NDT} determination implies already some conservatism in the approach. For the adjustment of the limit curve in the irradiated state the ΔT_{41J} criterion is used as determined from Charpy impact testing (mean curve). The conservatism in this procedure has been demonstrated within research programs where fracture mechanics, drop-weight and Charpy specimens were irradiated in test reactors and even in power reactors [24, 25]. However, recent results from the United States "Heavy Section Steel Irradiation" (HSSI) program indicate that the margin between actual fracture toughness values and the predicted fracture toughness on the basis of the ΔT_{41J} shift shrinks to zero [26]. This does not directly affect the safety of a plant because of a variety of other conservative assumptions but points out the necessity of a thorough evaluation of data, in particular in the case of materials highly sensitive to neutron irradiation.

Other factors in the assessment of the plant lifetime are of equal or even greater importance. During the design phase, only the specified chemical composition of the steel is available to estimate the sensitivity of the material against neutron irradiation. With actual data from quality assurance testing an adjustment can be made. With these data the change in transition temperature (ΔT_{41J}) and the drop in upper shelf (ΔUSE) can be determined from design curves, as presented for example in the United States Regulatory Commission Regulatory Guide (US Reg. Guide) 1.99 or the German KTA 3203 (KTA, Regelwerk für kerntechnische Anlagen). These design curves have been evaluated on the basis of test reactor irradiation experiments in the past and have been updated recently with results from surveillance testing, supported by theoretical models accounting for metallurgical processes responsible for changes in the sub-microstructure.

AT this time two diverse approaches exist. The US Code favours the combination of copper and nickel as being responsible for material degradation [13] whereas the trend curves in Germany [2] and in the ex-USSR [27] include copper and phosphorus. In the French approach copper, phosphorus and nickel is proposed [28]. In Japan an even complexer correlation between chemical composition and shift in transition temperature is being developed [29]. The contribution of nickel is still under discussion but has not been adopted in the Codes in general. Accepting that the effect of nickel is valid, this can be of special importance in considering the weld material because its nickel content is usually higher than that of the base material. In Fig 14 some typical design curves for ΔT_{41J}, which were or are in use are compared.

The change in transition temperature and upper shelf energy due to neutron irradiation is important to judge the sensitivity of the material. More importantly, however, for the safety analysis are the absolute values of the reference temperature and the upper shelf energy. During operation of a reactor, plant specific data becomes available from surveillance testing. That data can replace or will replace the design life assumptions depending on the amount of actual degradation in comparison with the data taken from the design curves.

The lay out of the surveillance program is therefore an essential point in the design phase (see chapter 8). To account for neutron spectrum and dose rate (neutron flux) effects, the location of the capsules in relation to the vessel wall has to be chosen adequately. A lead factor (ratio of neutron flux at capsule location and peak fluence at vessel wall) of 3-5 is recommended or required. This "close to wall irradiation" provides data which can be transferred reliably to assess the RPV wall material state (compare chapter 13).

6 Material limitations for pressurized thermal shock (PTS)

The vessel behavior under thermal shock loading is essentially controlled by the upper shelf toughness of the material with respect to ductile crack initiation and stable crack growth and by the nil ductility transition temperature (RT_{NDT} adjusted) with respect to brittle crack initiation.

The theoretical basis for fracture mechanics analyses in the linear elastic and the elastic-plastic regime has been provided to determine the load paths during PTS events for individual plants. Efforts, however, were undertaken to evaluate material limitations from a more generalized point of view. A series of component failure interactions was investigated for different plants from which an upper limit of transition temperature could be established, the so called PTS-screening criterion [29]. For circumferential welds the adjusted reference temperature may not exceed 149 °C, for base material and axial welds, this value amounts to 132 °C.

In this case and when the upper shelf energy does not drop below 68 J, no individual safety analysis has to be performed. This screening criterion summarizes the theoretical linear elastic fracture mechanics models, the warm prestress effect and a validation of the fracture mechanics concepts for crack initiation and crack arrest by large scale experiments. In other Codes, besides the U.S. Code, this generalized screening criterion has not yet been adopted.

Extensive R & D work in the past was related to PTS loading situations as the most critical load paths for the RPV. In general, the underlying fracture mechanics concepts could be validated not only in the linear elastic regime but also in the elastic plastic regime using the J-integral. With respect to the definition of crack initiation toughness, however, different methods and opinions still exist which lead to remarkably different toughness values (see chapter 5). Under certain assumptions the stable crack growth behavior of components can be described. This has been demonstrated in PTS experiments with thick walled hollow cylinders [31, 32]. On the one hand the crack resistance curve (J as an function of Δa) of the material was determined with a compact tension specimen (CT 25 mm). On the other hand, the driving force J was calculated for the component under the specific test conditions (load, temperature, time) as shown in Fig 15. Under the applied test conditions stable crack extension occurred, the amount of which could be derived from the crack resistance curve of the CT-specimes. Studies with materials of low upper shelf toughness and high transition temperature comparable to materials degraded by neutron irradiation to validate the fracture mechanics concept, Fig 16, are still being continued.

7 Preventive measures to cope with in-service material degradation under severe loading conditions

In spite of efforts to design vessels to meet the harsh nuclear environment, additional steps were necessary to minimize material degradation and to mitigate loading conditions in the plant. Therefore measures to cope with neutron irradiation and severe loading situations have been carried out in the past successfully for different nuclear power plants, mainly for older plants the materials of which are particularly sensitive to neutron irradiation. Three separate courses of action were taken [33] which will be explained in more detail from the German point of view:

- reduction of neutron flux to reduce design life fluence

- enhanced non destructive examination to limit the flaw size to be postulated

- mitigation of thermal shock loading.

7.1 Flux reduction

Advanced computer codes and a more detailed modelling of the geometry have yielded a higher maximum flux at the RPV wall when compared with the computations performed in the mid sixties. This, coupled with increased safety requirements, has made it necessary to reduce the flux in order to reach the design lifetime. Firstly burned-up fuel elements were arranged at the outer core edges, but later on dummy fuel elements were inserted at specific locations, Fig 17. This mitigation method was also introduced in other reactors [34]. By this means it was possible to reduce the neutron flux and thus the design life fluence drastically, in some cases even without lowering the reactor power.

7.2 Non destructive examination

According to the Codes the stress calculation for emergency conditions must not consider the 1/4 T flaw but a reduced flaw size which can be justified by the efficiency of the NDE techniques applied in the individual plant. Large efforts and progress have been made in recent years in the development of measuring equipment and data acquisition systems for flaw detection and sizing [35, 36]. The techniques have been verified and validated on a series of plates, forgings, small scale and full scale vessels. It is now extremely unlikely that a surface flaw of 5 mm depth will be missed. For the safety assessment a safety factor of two is required for the flaw size, therefore a flaw depth of 10 mm is commonly used in calculations. It was recognized that extensive NDE may be required also in the future. Therefore the design of the pressure vessel and the vessel internals must provide access to the critical areas of the RPV for non destructive testing equipment. In one case in Germany a special manipulative system had to be developed which was fed in the 60 mm gap between the thermal shield and the RPV to facilitate NDE of the core belt line region.

7.3 Mitigation of thermal shock loading

Calculations of the thermal shock load paths have clearly shown the influence of temperature of the water being injected during ECC, Fig 18. As one of the first steps to mitigate PTS impact on the RPV, the cooling water in some power plants was preheated to 30 °C and kept at that temperature constantly. In the future it is intended that the water will be preheated up to 50 °C. As a second step for plants with high design life (DL) fluence, additional modifications were made to alter the cooling water to be fed into the hot leg. This provides on the one hand a certain degree of mixing and thus a further increase in temperature.

On the other hand, the water does not pass the pressure vessel wall directly. Extensive studies [37] have demonstrated that even under hot leg water injection the core can be cooled sufficiently. This mitigation approach requires consideration in vessel design.

7.4 Annealing

Extensive studies have been performed with respect to annealing of a RPV to remove the effects of neutron irradiation on mechanical properties. Depending on the embrittlement mechanisms (see chapter 10) a high percentage of recovery occurs at 450 to 480 °C. Annealing of a RPV is only considered in case of highly sensitive materials and high DL fluences. Those materials, however, include the possibility of a remanent transition temperature shift after annealing. For the ex-USSR steel 15Kh12MFA used in WWER 440 reactors a remaining shift of 20 K is considered to which a safety margin of additional 20 K is added. Irradiation experiments with a high copper, high phosphorus, high nickel weld material have shown that high shift in transition temperature and a large drop in upper shelf energy occurs, Fig. 19. After annealing at 450 °C for 168 hours the upper shelf had completely recovered, but the remaining shift amounts to about 80 K. Fracture toughness data of this material give clear evidence that the shape of the K_{ic} curve will not be maintained in the highly embrittled state as assumed in the Code, Fig. 20. This has already been indicated by other irradiated weld materials, Fig. 21 and specially heat treated base material to simulate irradiation embrittlement, Fig. 22 [38].

Annealing of RPVs has been mainly considered for reactors of the WWER 440 type with its high fluence. Ten WWER 440 reactors have been annealed by 1991 [39]. In several countries feasibility studies for RPV annealing have been carried out on the basis of results of annealing behaviour studies. In Germany the licensing authorities have required a "stand by" full size annealing device for one particular PWR vessel in the late nineteen seventies [33]. At that time annealing was thought to be necessary for the particular reactor as a redundant measure. In the meantime, detailed fracture mechanics analyses in conjunction with other plant specific mitigation measures, such as flux reduction, preheating of cooling water and hot leg water injection have shown that annealing does not need to be considered for this particular vessel.

8 Summary

The generally increased safety requirements provided the impetus for a more detailed evaluation of the pressure vessel behaviour in some areas. Progress has been made in analysing transient conditions and to evaluate out the most severe load paths on a fracture mechanics basis. In this respect the expansion of the fracture mechanics analysis from the linear elastic regime into the elastic plastic regime was a decisive step towards describing component behaviour over the entire temperature regime. The better understanding of in-service degradation mechanisms and their quantification gave further elucidation of the conservatism in the safety analysis.

From the consequent research in this field together with feed-back from plant performance and surveillance results, implications can be derived for the design of new vessels (material optimization, increase in water gap and thus decrease in resulting neutron exposure) and for mitigation measure (ease of transient loading, reduction of neutron exposure) with regard to older plants. In this respect the pressurized thermal shock (PTS) event plays the most important role. Associated with this loading condition the defect size to be postulated and the reliable knowledge on the material state are the crucial parameters on which the life assessment is based.

Ageing parameters others than neutron irradiation, have not considered in this chapter. Thermal ageing has minor effect at LWR operating temperature and corrosion assisted crack growth is an area which deserves separate consideration.

References

1. "Standard Practice for Conducting Surveillance Tests for Light-Water Cooled Nuclear Power Reactor Vessels" American Society for Testing Materials ASTM E 185,1982

2. "Uberwachung der Strahlenversprodung von Werkstoffen des Reaktordruckbehalters von Leichtwasserreaktoren" Sicherheitstechnische Regel, Kerntechnischer Ausschuss (KTA 3203), Cologne, Germany, 1984

3. "Komponenten des Primarkreises von Leichtwasserreaktoren Teil 2: Auslegung, Konstruktion und Berechnung" Sicherheitstechnische Regel, Kerntechnischer Ausschuss (KTA 3201.2), Cologne, Germany, 1984

4. Kussmaul, K. Basis Safety Concept Rules out Possibility of Catastrophic Failure Nuclear Engineering International (Dec. 1984) pp. 41 - 46

5. Kussmaul, K., W. Stoppler and R. Sinz Development of Material and Welding Processes for Nuclear Application in the Federal Republic of Germany, Intern. Conference on "Welding Technology for Energy Application",May 16-19 1982, Gatlinburg,TN,USA, (Compiled by S.A. David and G.M. Slaughter) Oak Ridge National Laboratory,USA,1992,

6. Kussmaul, K.., J. Fohl and E. Roos Application of Advanced Material, Design and Computation Technologies to Enhance Safety Reliability and Availability IAEA Specialists' Meeting on "Recent Trends in Development of Reactor Circuit Technology" 25 - 28 Nov. 1985, Madrid, Spain, Pressure Vessel and Piping Vol. 25 (1986) pp 185 - 215

7. Kussmaul, K. and Föhl, J.
The Effect of Neutron Irradiation and Measures to Assure the Safety of the Reactor Pressure Vessel,
International Symposium on "Pressure Vessel Technology and Nuclear Codes and Standards", MPA Stuttgart
April 19-21, 1989, Seoul, Republic of Korea

8. Lowe, A.L. and Pegram, I.W.
Improved Correlations for Predicting the Effects of Neutron Radiation on Linde 80 Submerged-Arc Weld Metals
"Effects of Radiation on Materials" (Editors:
N.H. Packan/R.E. Staller/A.S.Kumar)
ASTM-STP 1046 (1990) pp 234-252

9. Pellini, W.S.
Evolution of Engineering Principles for Fracture-Safe Design of Steel Structures
Naval Research Laboratory (NRL) Report 6957 (1969),
Washington, D.C., USA

10. American Society of Mechanical Engineers (ASME)
Boiler and Pressure Vessel Code, Section III Article
NB 2000 "Material", 1986

11. "Komponenten des Primarkreises von Leichtwasserreaktoren
Teil 1: Werkstoffe"
Sicherheitstechnische Regel, Kerntechnischer Ausschuss,
KTA 3201.1, 1979

12. United States Nuclear Regulatory Commission
"Rules and Regulations", Title 10, Codes of Federal Regulations (CFR), Part 50, App. G "Fracture Toughness Requirements", 1986

13. United States Nuclear Regulatory Commission, Regulatory Guide 1.99 "Radiation Embrittlement of Reactor Vessel Materials"
Revision 1 and 2, 1977 and 1978

14. American Society of Mechanical Engineers (ASME)
Boiler and Pressure Vessel Code, Section III App. G "Protection Against Nonductile Failure", 1986

15. Iskander, S.K., A. Sauter and J. Fohl
Reactor Pressure Vessel Structural Implication of
Embrittlement to Pressurized-Thermal-Shock Scenario
"Radiation Embrittlement of Nuclear Reactor Pressure
Vessel Steels - An International Study" (Editor:
L.E. Steele)
ASTM STP 909 (1986) pp 163 - 176

16. Kussmaul, K. and A. Sauter
Equipment Simulation to Investigate Overcooling Events
in Light Water RPV's
Nuclear Engineering and Design Vol. 87 (1985)
pp 313 - 327

17. Cheverton, R.D. et al
Effect of Temperature Dependence of Material Properties
an the Calculated Values of Ki
NUREG/CR 2141 Vol. 4 (ORNL/TM 8252) Oak Ridge National
Laboratory April 1982 pp 84-87

18. Pellisier-Tanon, A., P. Sollogaub and B. Houssin
"Crack Initiation and Arrest in an SA 508 class-3
Cylinder under Liquid Nitrogen Thermal-Shock Experiment"
7th Intern. Conference on Structural Mechanics in
Reactor Technology (SMiRT), Chicago,USA (1983),
North-Holland, Amsterdam,Netherlands
Vol. G/H, pp 137 - 142

19. Sauter, A., R.D. Cheverton and S.K. Iskander
"Modification of OCA-I for Application to a Reactor
Pressure Vessel with Cladding at the Inner Surface".
Report NUREG/CR-3155 ORNL/TM-8649, Oak Ridge National
Laboratory, USA, May 1983

20. American Society of Mechanical Engineers (ASME) Boiler
and Pressure Vessel Code Section XI A 5000, "Analysis",1986

21. Loss, F.J., R.A. Gray and J.R. Hawthorne
"Significance of Warm Prestress to Crack Initiation
During Thermal Shock"
NRL/NUREG Report 8165 (Sept. 1985)

22. Cottrell, A.
Warm Prestressing and fractures in Structural Steel,
Engineering Fracture Mechanics 28 (1987) No 5/6
pp 481-483

23. Hollstein, T., J.G. Blauel, R. Kienzler and G. Nagel
Use of Load Path Dependent Material Fracture Toughness
Values (WPS) in the Safety Analysis of RPV Stade
Nuclear Engineering and Design 94 (1986) pp 233-239

24. Klausnitzer, E.N., A. Gerscha and Ch. Leitz
Irradiation Behavior of Nickel-Chromium-Molybdenum Type
Weld Metal
"Effects of Radiation on Structural Materials" (Editors:
J. A. Sprague/D.Kramer)
ASTM - STP 683 (1979) pp 267-277

25. Fohl, J., Ch. Leitz and D. Anders
Irradiation Experiments in the Testing Nuclear Power
Plant VAK
"Effects of Radiation on Materials" (Editors:
H.R. Brager/J. S. Perrin)
ASTM - STP 782 (1982) pp 520-549

26. Nanstad, R.K. et al.
Effects of Radiation on Kic Curves for High Copper Welds
"Effects of Radiation on Materials (Volume II)" (Editors:
N.H. Packan/R.E.Staller/A.S.Kumar)
ASTM -/STP 1046 (1990) pp 214-233

27. Tulyakov, G.A. et al.
Pressurized Water Reactor (PWR) Vessel Materials
Irradiation Resistance
IAEA-Specialists' Meeting on "Radiation Embrittlement of
Nuclear Reactor Pressure Vessel Steels"
26-28 Sept. 1990, Balatonfured, Hungary
ASTM STP 1170, American Society for Testing and Materials,
Philadelphia,1993

28. Petrequin, P.
Irradiation Embrittlement of Pressure Vessel Steels: A Review of Activities in France, "Radiation Embrittlement and Surveillance of Nuclear Pressure Vessels" (Editor: L.E. Steele)
ASTM STP 819 (1983) pp 29-52

29. Ishino, T., T. Kawakani, T. Hidaka, M. Satoh
The Effect of chemical Composition on Irradiation Embrittlement
14th MPA Seminar on "Safety and Reliability of Plant Technology", 6-7 Oct. 1988 Stuttgart, Germany
Nuclear Engineering and Design, May 1990,,v.119(2/3),P.139-148

30. United States Nuclear Regulatory Commission "Rules and Regulations" Title 10 Code of Federal Regulation (CFR) Part. 50.61
"Fracture Toughness Reguirements for Protection Against Pressurized Thermal Shock Events",1987

31. Kussmaul, K. and J. Fohl
Radiation Effects on the Integrity of Light Water Reactor Pressure Vessels
3rd Int. Conference on "Environmental Degradation of Materials in Nuclear Power Systems - Water Reactors" Aug. 30 - Sept. 3, 1987, Traverse City, Michigan, USA
G.J.Theus and J.R.Weeks, Eds., The Metallurgical Society,Warrendale,PA,1988

32. Jovanovic, A., A. Sauter and A.C. Lucia
Some Current Issues in the PTS Research
Nuclear Engineering and Design 112 (1989) pp 259-278

33. Kussmaul, K.
Specific Problems of Reactor Pressure Vessels Related to Irradiation Effects
"Radiation Embrittlement and Surveillance of Nuclear Reactor Pressure Vessels: An International Study" (Editor: L.E. Steele)
ASTM - STP 819 (1983) pp 86-99

34. Ahlstrand, R., Törrönen, K., Valo, M. and Bars, B.
Surveillance Programs and Irradiation Embrittlement
Research of the Loviisa Nuclear Power Plant, "Radiation
Embrittlement of Nuclear Reactor Pressure Vessel Steels"
(Editor: L.E. Steele)
ASTM-STP 909, 1986, pp 55-89

35. Mletzko, U., Kussmaul, K., Herkenrath, H., and Crutzen, S.
Full Scale ISI within the Full Scale Action of PISC III
Post SMiRT Conference on "Assuring Structural Integrity
of Steel Reactor Pressure Boundary Components"
Aug. 26-28, 1991, Taipei, Taiwan
Nuclear Engineering Design, Vol. 125, 1991

36. Dykas, E.R. and Terkune, J.H.
An Advanced Ultra Sonic System for BWR Vessel Weld
Inspection
Post-SMiRT Conference on "Assuring Structural Integrity
of Steel Reactor Pressure Boundary Components"
Aug. 26-28, 1991, Taipei, Taiwan
Nuclear Engineering Design, Vol. 125, 1991

37. Weiss, P.A. and Hertlein, R.J.
UPTF Test Results: First Three Separate Effect Tests
Nuclear Engineering and Design 108, 1988, pp 249-263

38. Kussmaul, K. and Föhl, J.
The Effects of Irradiation on the Integrity of Light
Water Reactor Pressure Vessels, "Environmental
Degradation of Materials in Nuclear Power Systems Water"
Reactors (Editor: G.H. Theus, J.R. Weeks)
The Metallurgical Society, 1988

39. Dragunov, Yu.G. et al.
Practical Experience of Annealing to Extend WWER Reactor
Life Time
11th International Conference on "Structural Mechanics in Reactor
Technology (SMiRT) Session F12
Aug. 18-23, 1991, Tokyo, Japan, Atomic Energy Society of Japan, 1991

Fig. 1: Elements of the DETERMINISTIC safety approach in the BASIS SAFETY CONCEPT

Fig. 2: Comparison of main RPV dimensions in the core belt line region

Fig. 3: Comparison of gross dimensions of different reactor pressure vessels

Fig. 4: Typical size of water gap and neutron flux at wet surface of BWR and PWR reactor pressure vessels

Fig. 5: Determination of reliable data on materials and stresses for life assessment

Fig. 6: Pressure/temperature limit curve based on the reference temperature RT_{NDT} (modified Porse Diagram)

Fig. 7: Fracture Toughness of the materials and load path for start up, normal operation and shut down

Fig. 8: Example of pressure and temperature as a function of time for small steam line break (leak area 1960 mm^2)

<u>Fig. 9</u>: Stress intensity of a circumferential crack resulting from transient as shown in Fig. 8

<u>Fig. 10</u>: Stress intensity of an axial crack during resulting from transient as shown in Fig. 8

<u>Fig. 11</u>: Characteristic information needed for the safety assessment of an emergency core cooling event; circumferential flaw, pressure/temperature history according to Fig. 8

a) temperature across the wall
b) stress intensity depending on crack depth
c) stress intensity as a function of time

<u>Fig. 12</u>: Determination of crack initiation and crack arrest events during ECC (schematically) on a fracture mechanics basis in the linear elastic regime

<u>Fig. 13</u>: Schematic demonstration of "fracture" and "no fracture" load paths as referred to the "warm prestress effect"

<u>Fig. 14</u>: Comparison of different internationally applied design curves to predict the shift in transition temperature as a function of neutron exposure

Fig. 15: Example of a PTS-Test for Validation of fracture mechanics concepts in the elastic-plastic regime

Fig. 16: Materials used for validation of fracture mechanics analysis under PTS conditions

Fig. 17: Example of the effect of change in core loading to reduce the neutron flux at the RPV wall

Fig. 18: Influence of injection water temperature on the stress intensity during ECC

Fig. 19: Irradiation behaviour of highly sensitive weld material

Fig. 20: Fracture toughness of highly irradiated material (Cu = 0.37 %, P = 0.017 %, Ni = 1.23 %) in comparison with unirradiated data

Fig. 21: Fracture Toughness of high copper submerged arc weld in the unirradiated and irradiated state

Fig. 22: Fracture toughness of materials in conditions (chemical composition, forging and heat treatment) simulating the properties of irradiated material

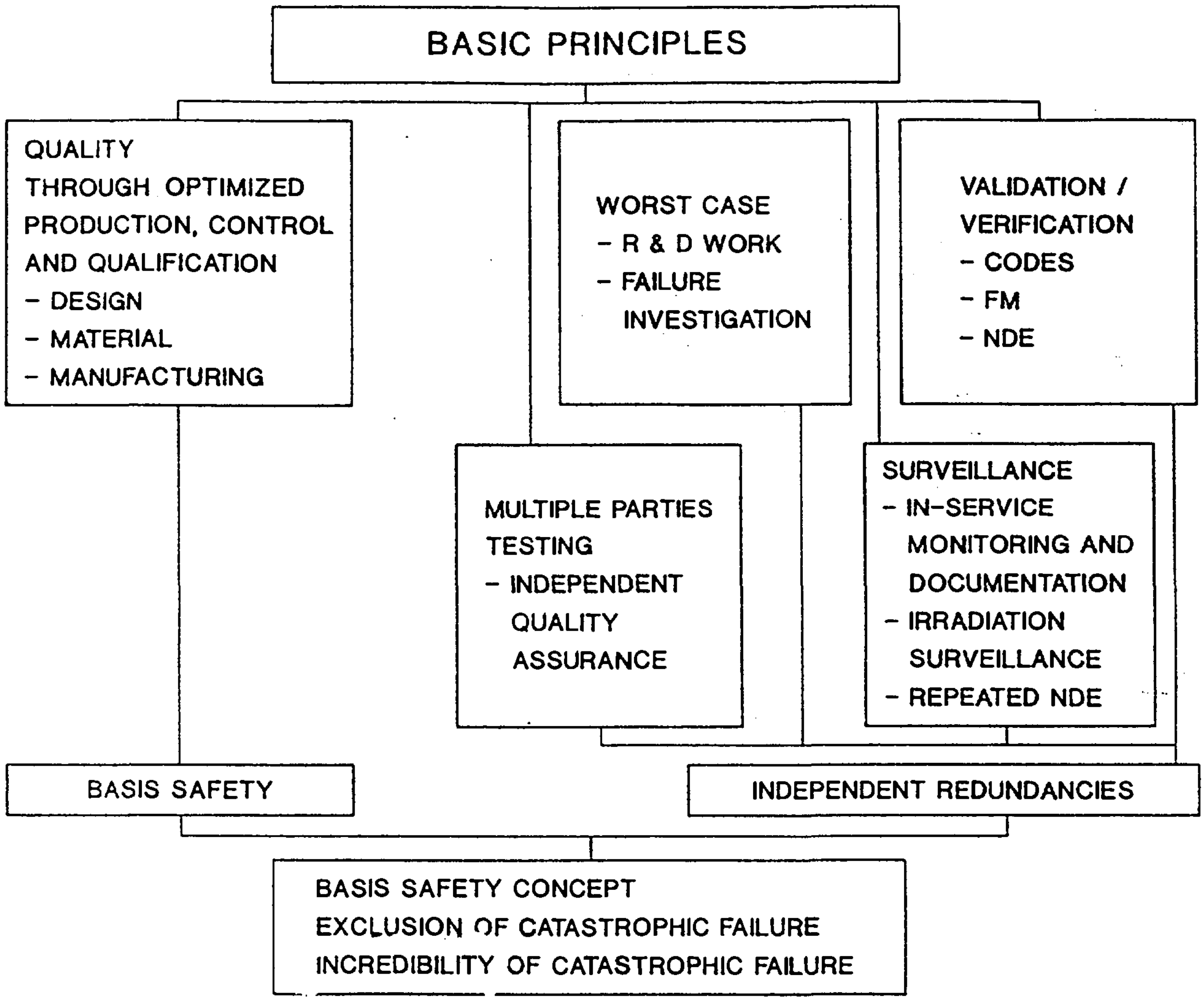
BASIC PRINCIPLES
QUALITY THROUGH OPTIMIZED PRODUCTION, CONTROL AND QUALIFICATION
- DESIGN
- MATERIAL
- MANUFACTURING
WORST CASE
- R & D WORK
- FAILURE INVESTIGATION
VALIDATION / VERIFICATION
- CODES
- FM
- NDE
MULTIPLE PARTIES TESTING
- INDEPENDENT QUALITY ASSURANCE
SURVEILLANCE
- IN-SERVICE MONITORING AND DOCUMENTATION
- IRRADIATION SURVEILLANCE
- REPEATED NDE
BASIS SAFETY
INDEPENDENT REDUNDANCIES
BASIS SAFETY CONCEPT
EXCLUSION OF CATASTROPHIC FAILURE
INCREDIBILITY OF CATASTROPHIC FAILURE

FIGURE 1

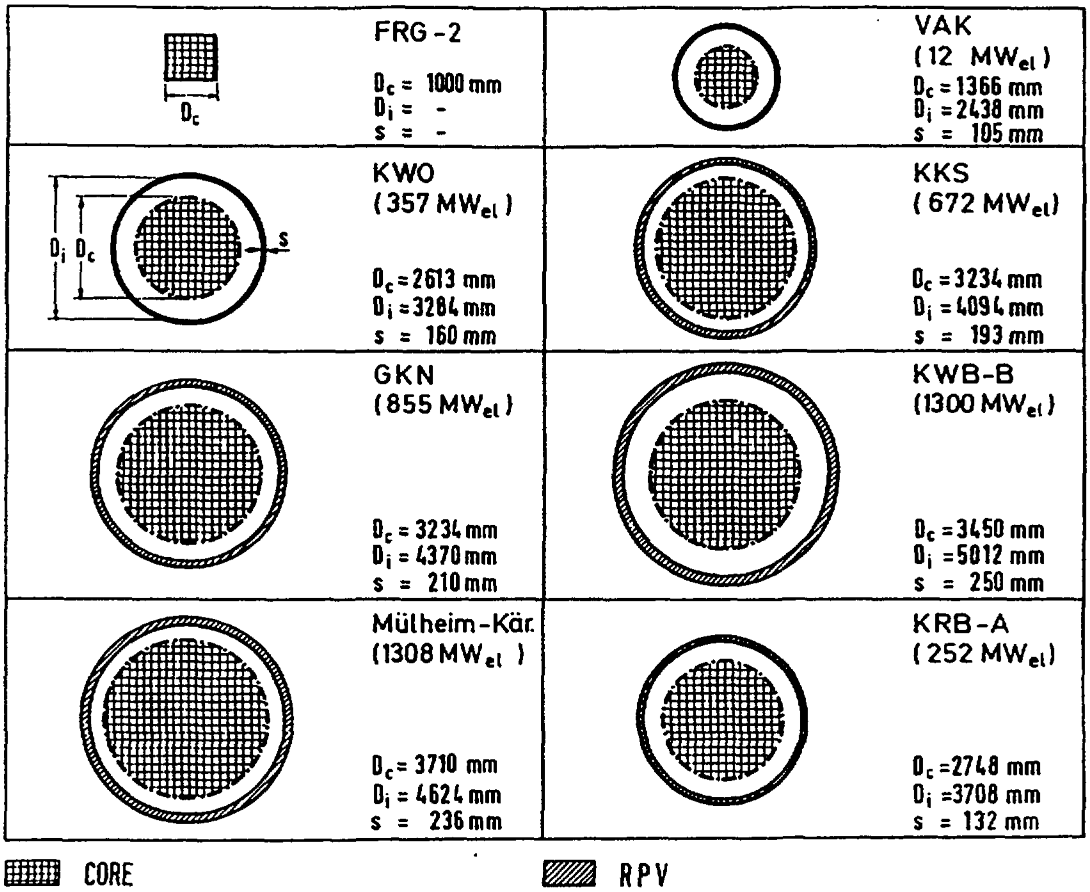
FRG - 2
Dc = 1000 mm
Di = -
s = -
VAK
(12 MWel)
Dc = 1366 mm
Di = 2438 mm
s = 105 mm
KWO
(357 MWel)
Di Dc
s
Dc = 2613 mm
Di = 3284 mm
s = 160 mm
KKS
(672 MWel)
Dc = 3234 mm
Di = 4094 mm
s = 193 mm
GKN
(855 MWel)
Dc = 3234 mm
Di = 4370 mm
s = 210 mm
KWB-B
(1300 MWel)
Dc = 3450 mm
Di = 5012 mm
s = 250 mm
Mülheim-Kär.
(1308 MWel)
Dc = 3710 mm
Di = 4624 mm
s = 236 mm
KRB-A
(252 MWel)
Dc = 2748 mm
Di = 3708 mm
s = 132 mm
CORE
RPV

FIGURE 2

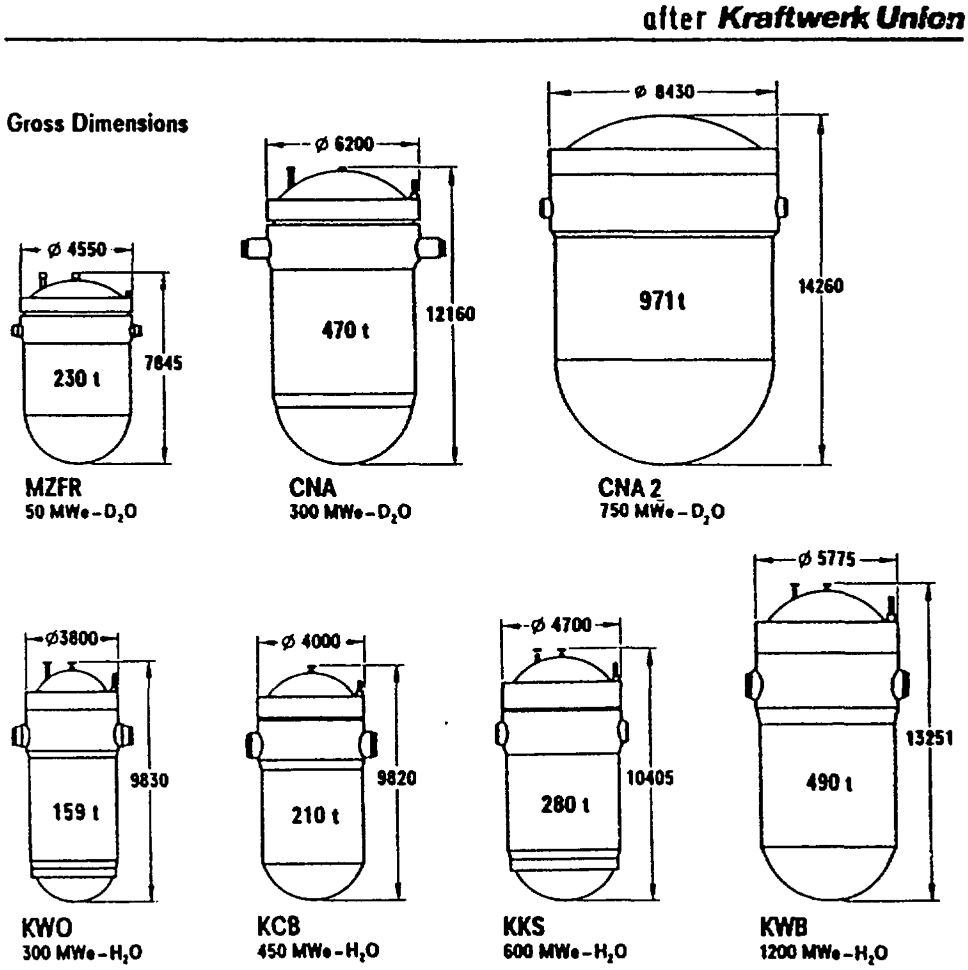
after Kraftwerk Union
Gross Dimensions
ø 4550
230 t
7845
MZFR
50 MWe - D_2O
ø 6200
470 t
12160
CNA
300 MWe - D_2O
ø 8430
971 t
14260
CNA 2
750 MWe - D_2O
ø3800
159 t
9830
KWO
300 MWe - H_2O
ø 4000
210 t
9820
KCB
450 MWe - H_2O
ø 4700
280 t
10405
KKS
600 MWe - H_2O
ø 5775
490 t
13251
KWB
1200 MWe - H_2O

FIGURE 3

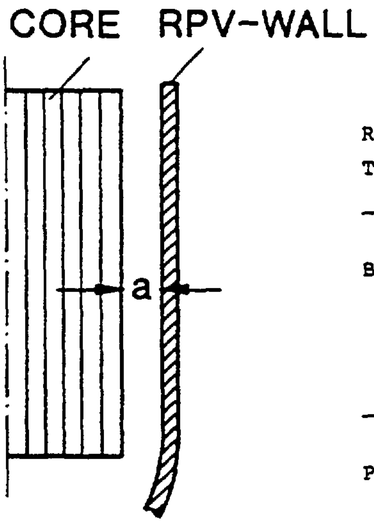

REACTOR TYPE	POWER (MW)	WATER GAP (mm)	n-FLUX $cm^{-2}\ s^{-1}$	DL-FLUENCE cm^{-2}
BWR	900	897	$1.2 \cdot 10^{9}$	$1.2 \cdot 10^{18}$
	1300	748		
	1316	972		
PWR	357	336	$3.5 \cdot 10^{10}$	$3.5 \cdot 10^{19}$
	672	430		$1.4 \cdot 10^{9}$
	855	568		
	1300	781		$5 \cdot 10^{18}$
	1308	456	$2 \cdot 10^{10}$	$2 \cdot 10^{19}$

FIGURE 4

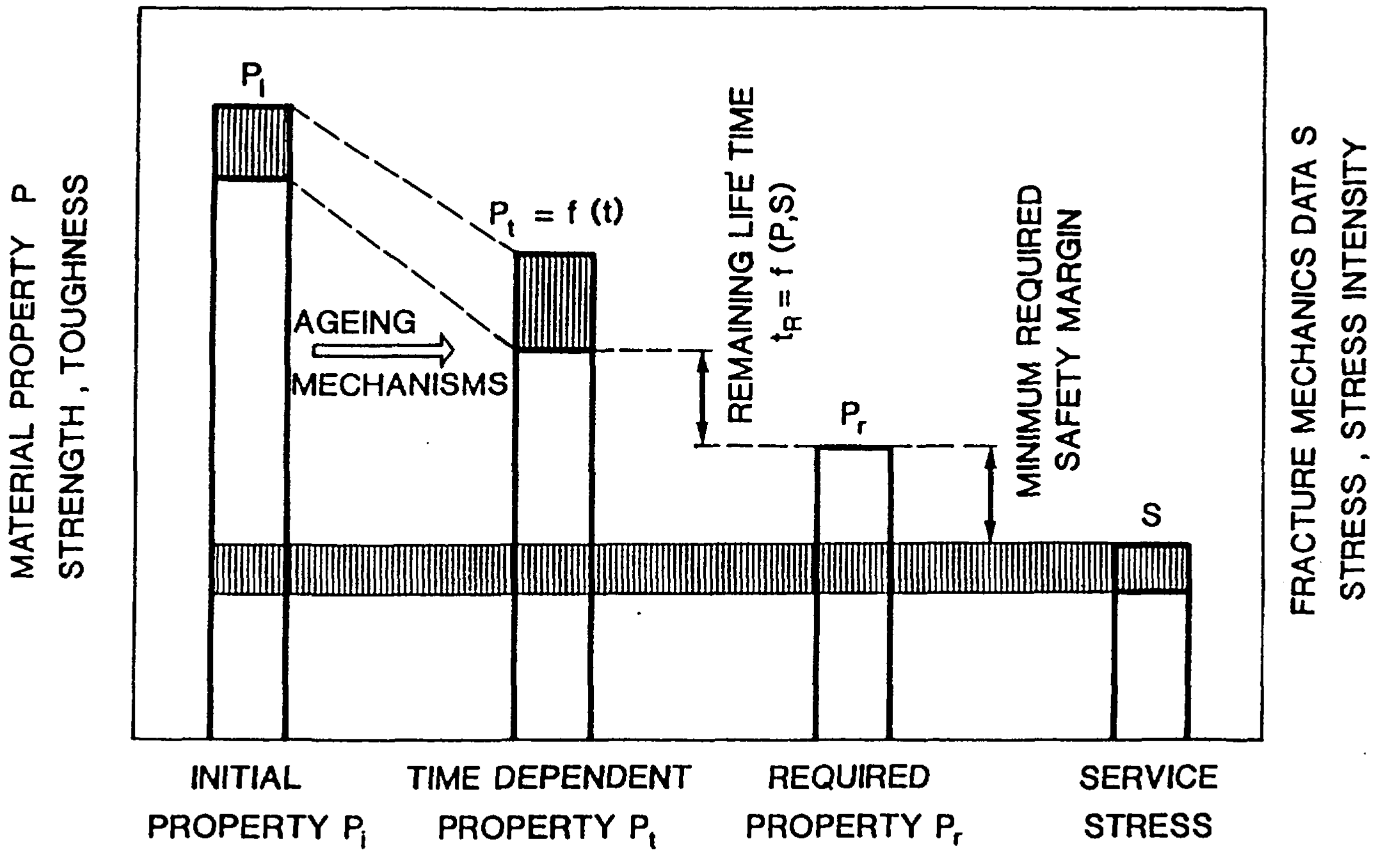
MATERIAL PROPERTY P
STRENGTH , TOUGHNESS
P
AGEING
MECHANISMS
P_t = f (t)
REMAINING LIFE TIME
t_R = f (P,S)
P_r
MINIMUM REQUIRED
SAFETY MARGIN
S
FRACTURE MECHANICS DATA S
STRESS , STRESS INTENSITY
INITIAL
PROPERTY P_i
TIME DEPENDENT
PROPERTY P_t
REQUIRED
PROPERTY P_r
SERVICE
STRESS

FIGURE 5

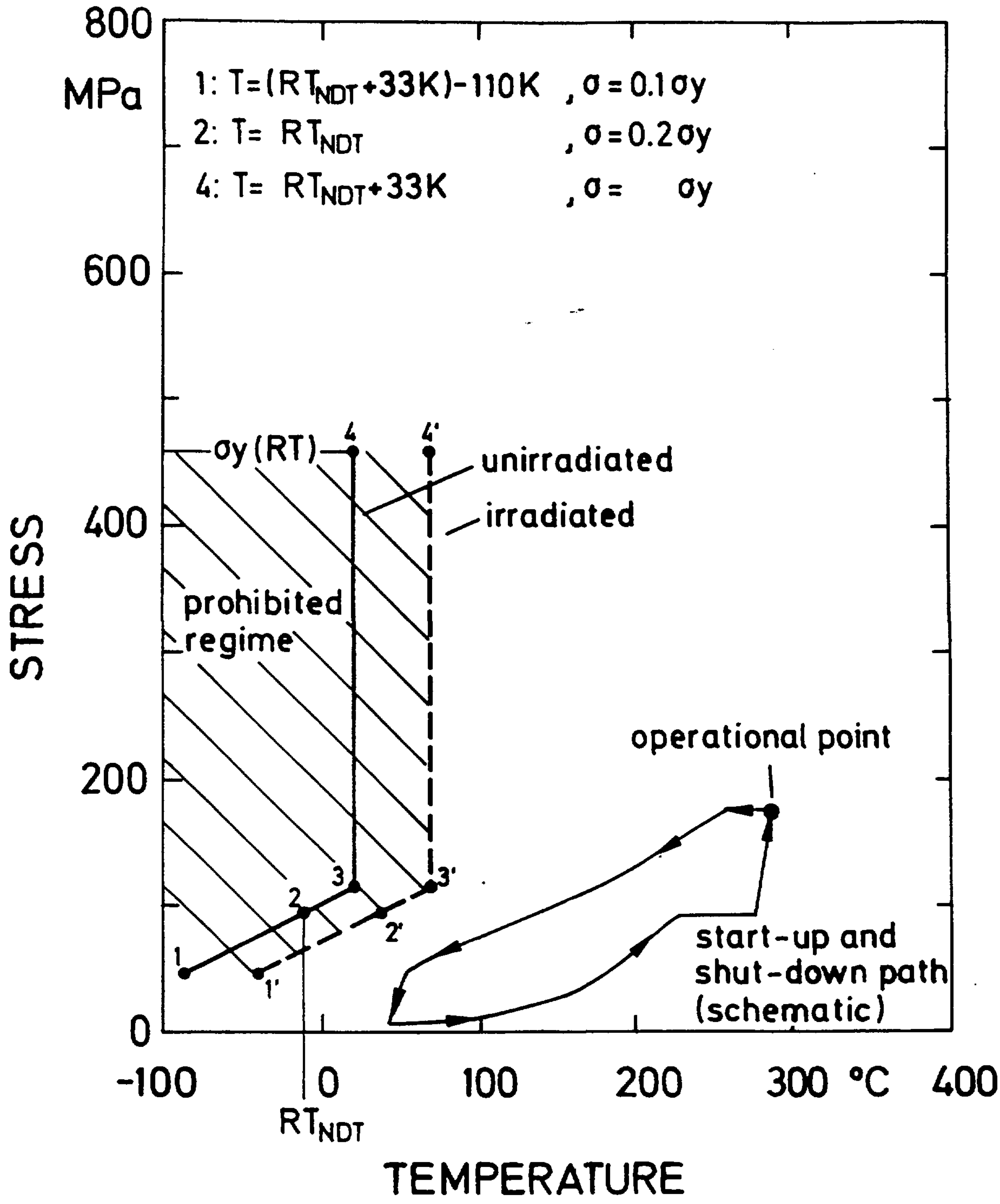
800
MPa
600
400
200
0
STRESS
1: T=(RT_NDT+33K)-110K , σ=0.1σy
2: T= RT_NDT , σ=0.2σy
4: T= RT_NDT+33K , σ= σy
σy (RT)
4
4'
unirradiated
irradiated
prohibited regime
operational point
3
3'
2
2'
1
1'
start-up and shut-down path (schematic)
-100
0
100
200
300 °C
400
RT_NDT
TEMPERATURE

FIGURE 6

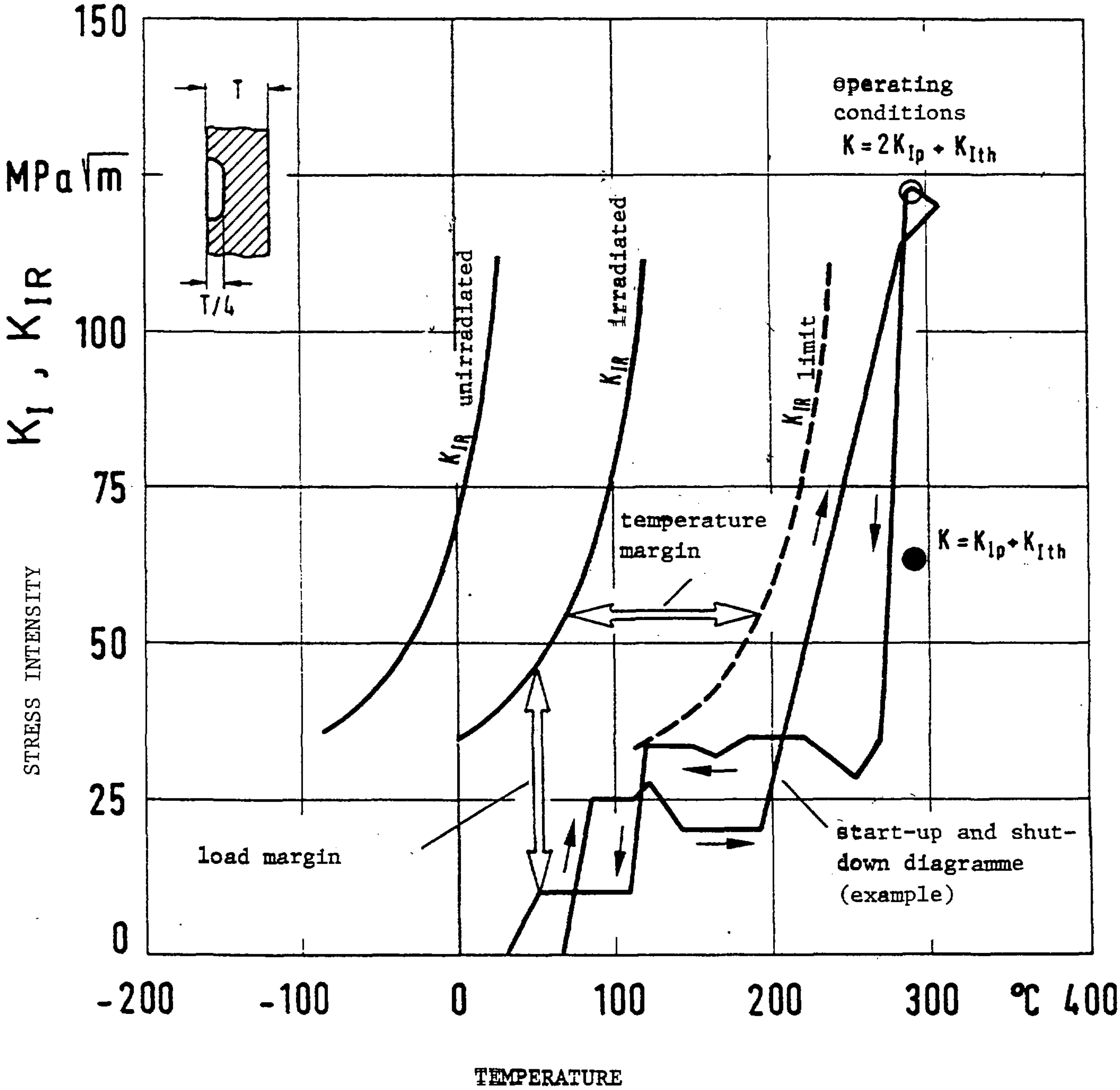
150
T
T/4
MPa √m
K_I , K_IR
100
75
50
25
0
STRESS INTENSITY
K_IR unirradiated
K_IR irradiated
K_IR limit
operating
conditions
K = 2 K_Ip + K_Ith
temperature
margin
K = K_Ip + K_Ith
load margin
start-up and shut-
down diagramme
(example)
-200
-100
0
100
200
300
°C 400
TEMPERATURE

FIGURE 7

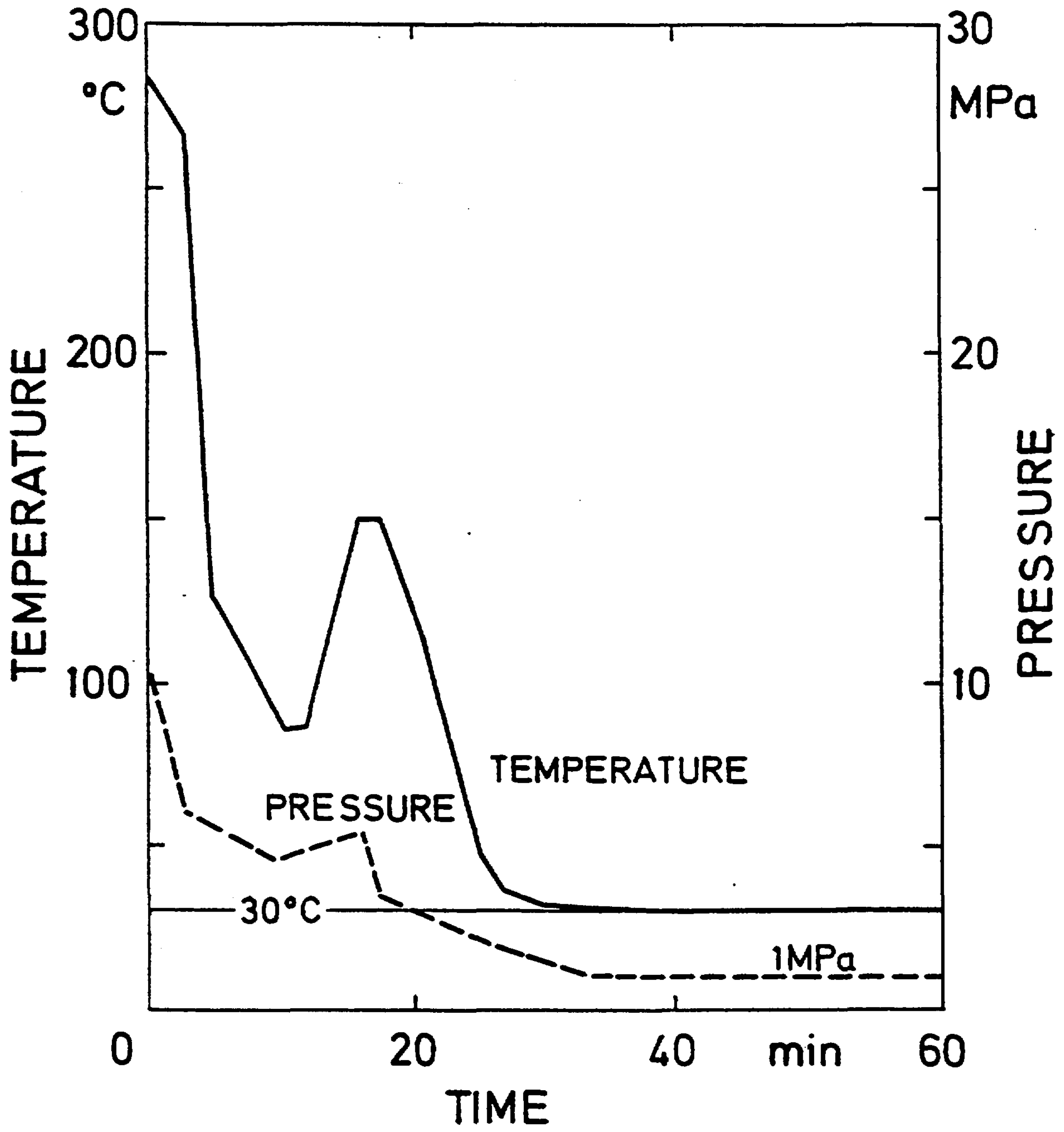
300
°C
200
100
TEMPERATURE
30
MPa
20
10
PRESSURE
TEMPERATURE
PRESSURE
30°C
1MPa
0
20
40
min
60
TIME

FIGURE 8

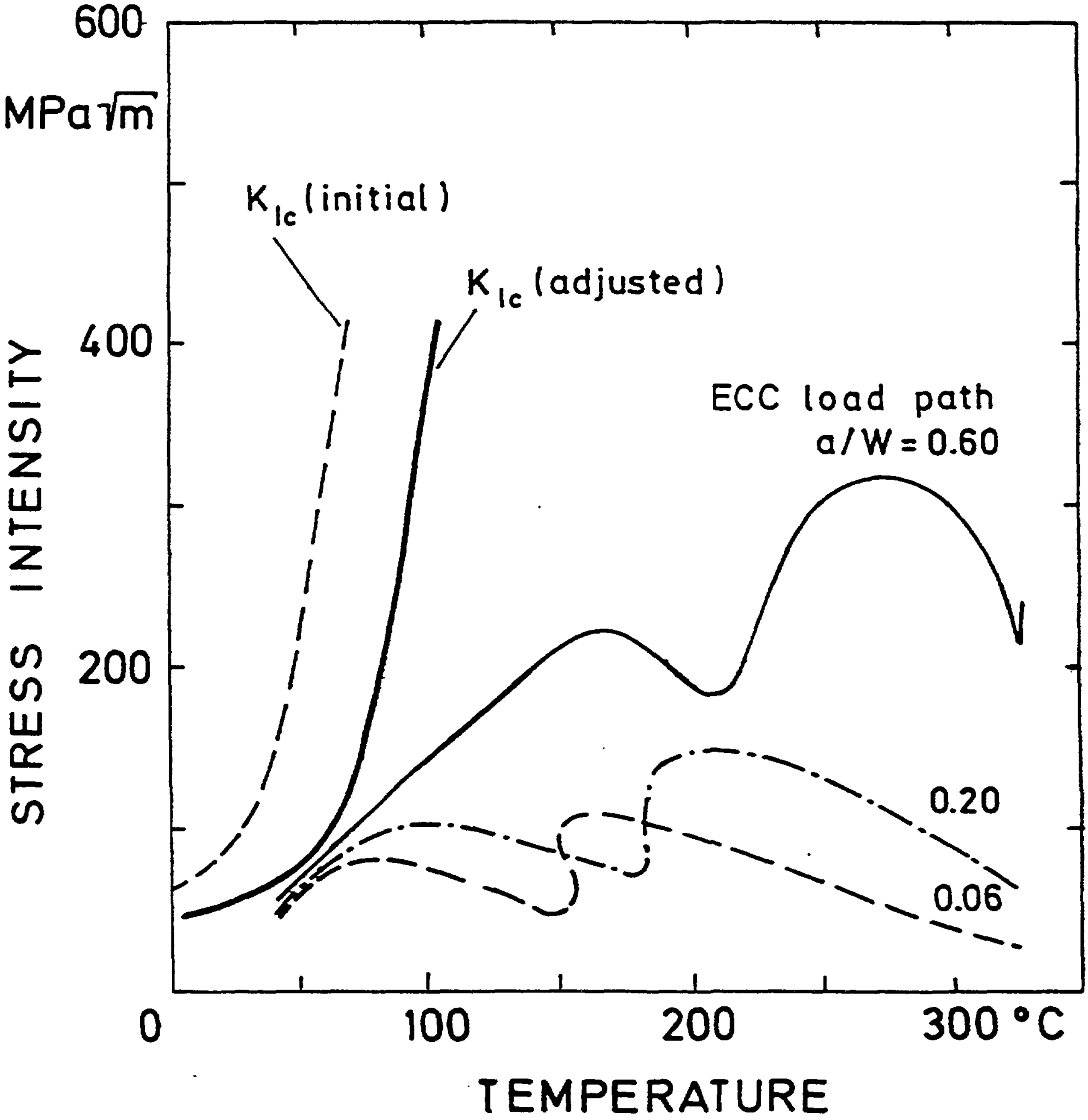

600
MPa√m
400
200
0
STRESS INTENSITY
K_{Ic} (initial)
K_{Ic} (adjusted)
ECC load path
a/W = 0.60
0.20
0.06
100
200
300 °C
TEMPERATURE

FIGURE 9

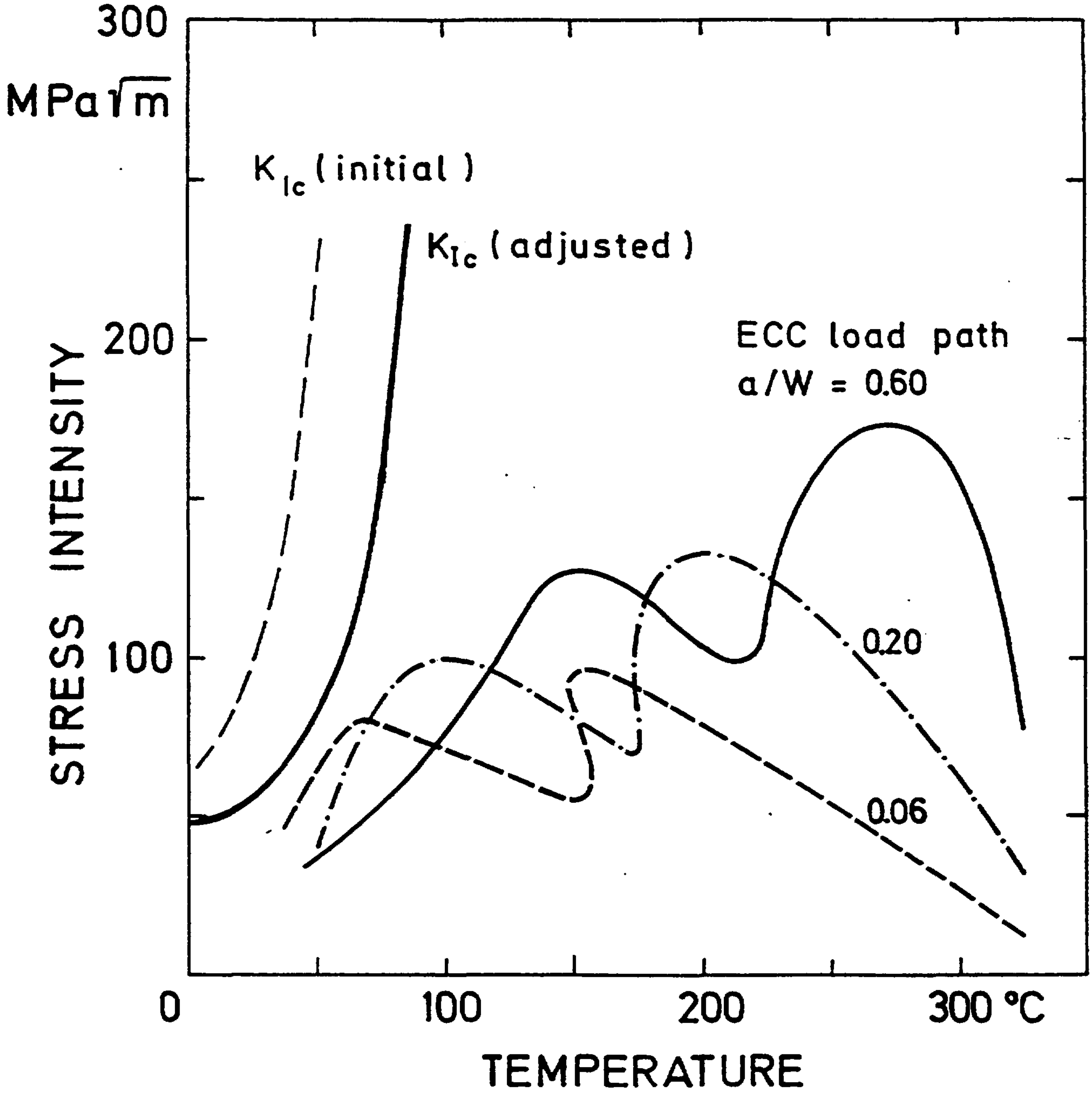

300
MPa√m
K_{Ic} (initial)
K_{Ic} (adjusted)
200
ECC load path
a/W = 0.60
STRESS INTENSITY
100
0.20
0.06
0
100
200
300 °C
TEMPERATURE

FIGURE 10

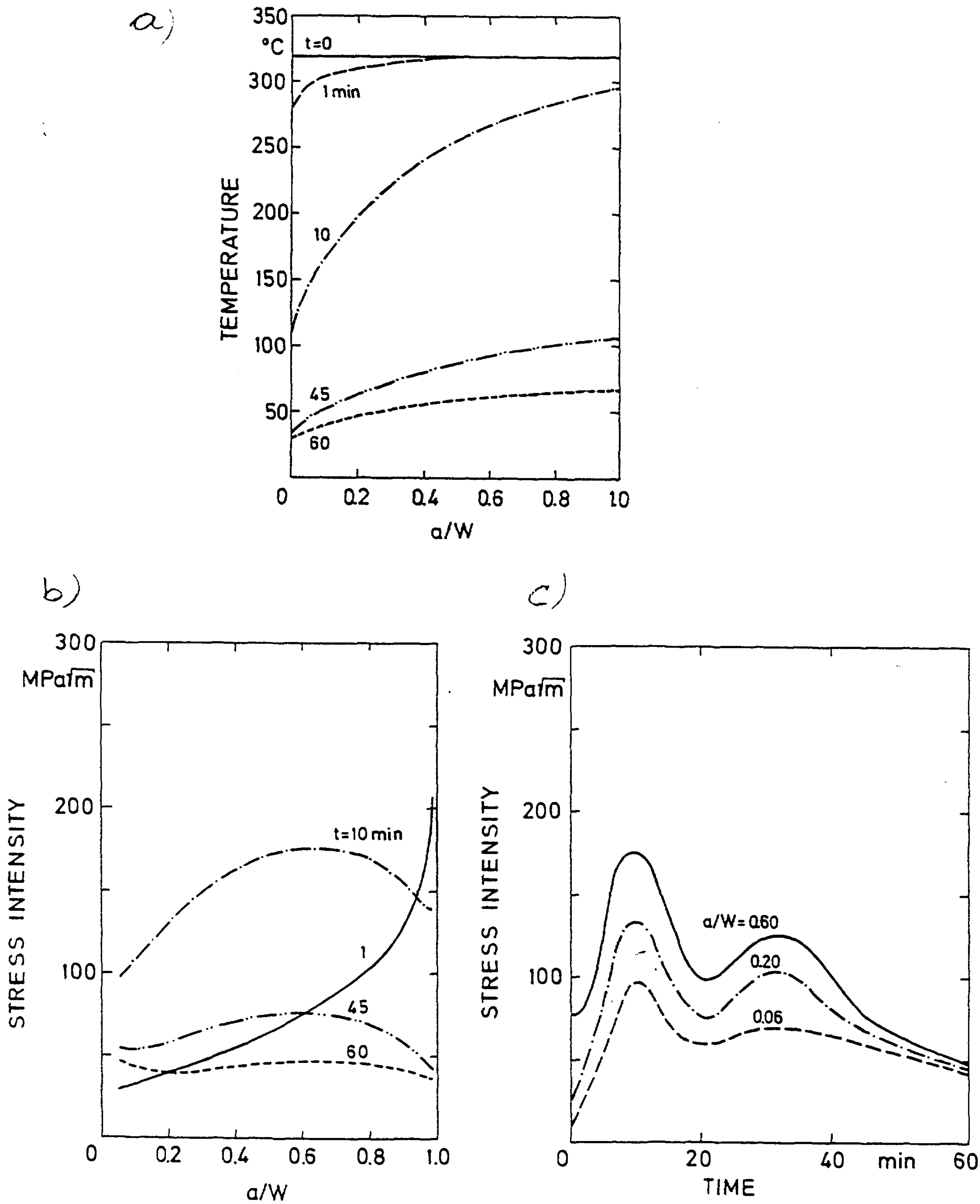
a)
350
°C
t=0
300
1 min
250
200
10
150
100
45
50
60
0
0.2
0.4
0.6
0.8
1.0
a/W
TEMPERATURE
b)
300
MPa√m
200
100
0
0.2
0.4
0.6
0.8
1.0
a/W
STRESS INTENSITY
t=10 min
1
45
60
c)
300
MPa√m
200
100
0
20
40
min
60
TIME
STRESS INTENSITY
a/W=0.60
0.20
0.06

FIGURE 11

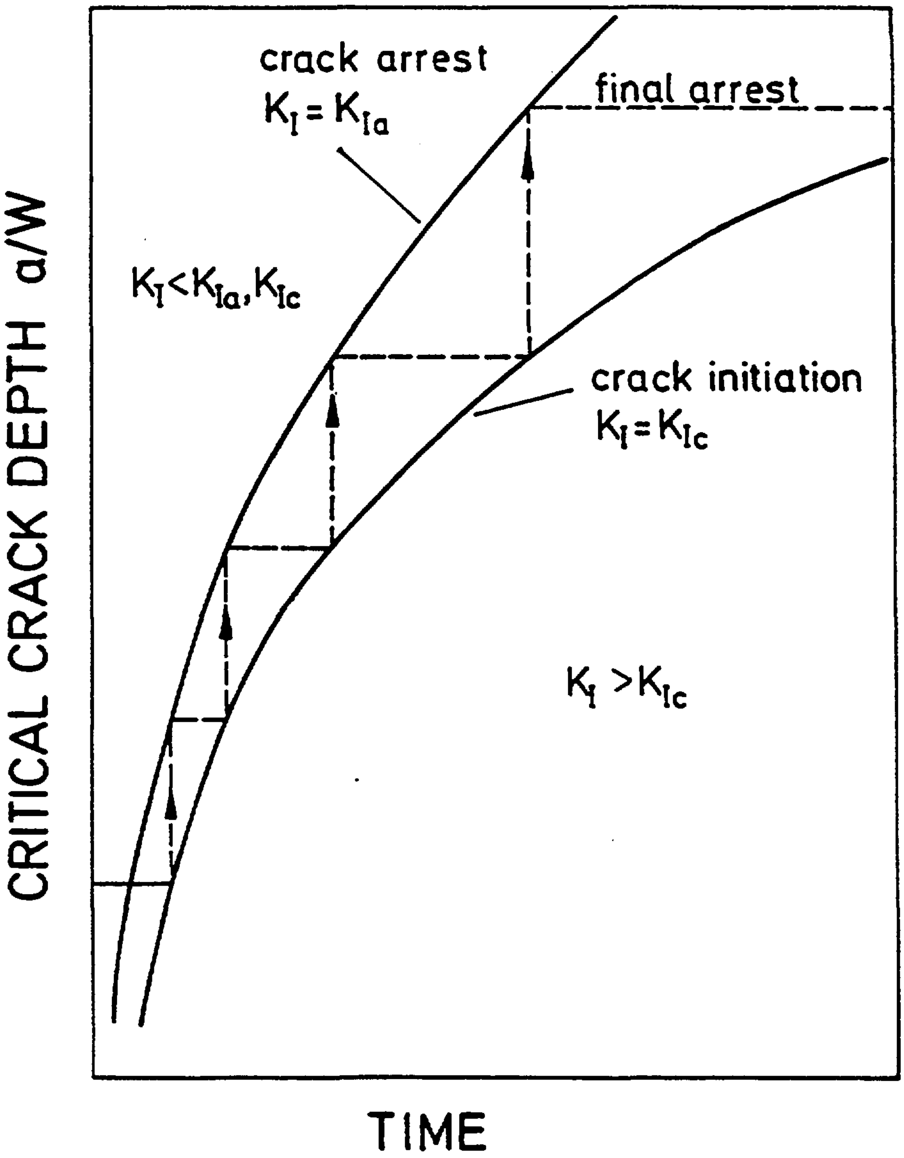
crack arrest
$K_I = K_{Ia}$
final arrest
$K_I < K_{Ia}, K_{Ic}$
crack initiation
$K_I = K_{Ic}$
$K_I > K_{Ic}$
CRITICAL CRACK DEPTH a/W
TIME

FIGURE 12

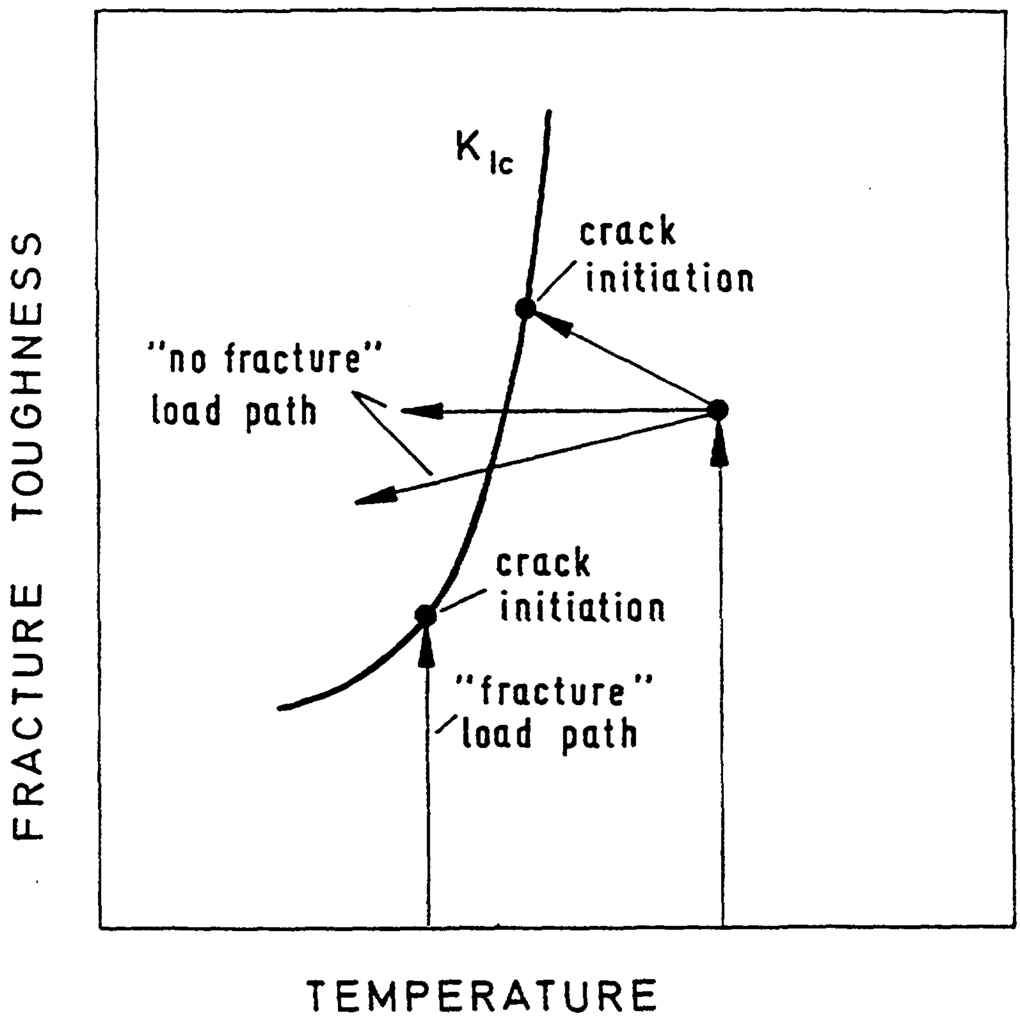

K_{Ic}
crack initiation
"no fracture" load path
crack initiation
"fracture" load path
FRACTURE TOUGHNESS
TEMPERATURE

FIGURE 13

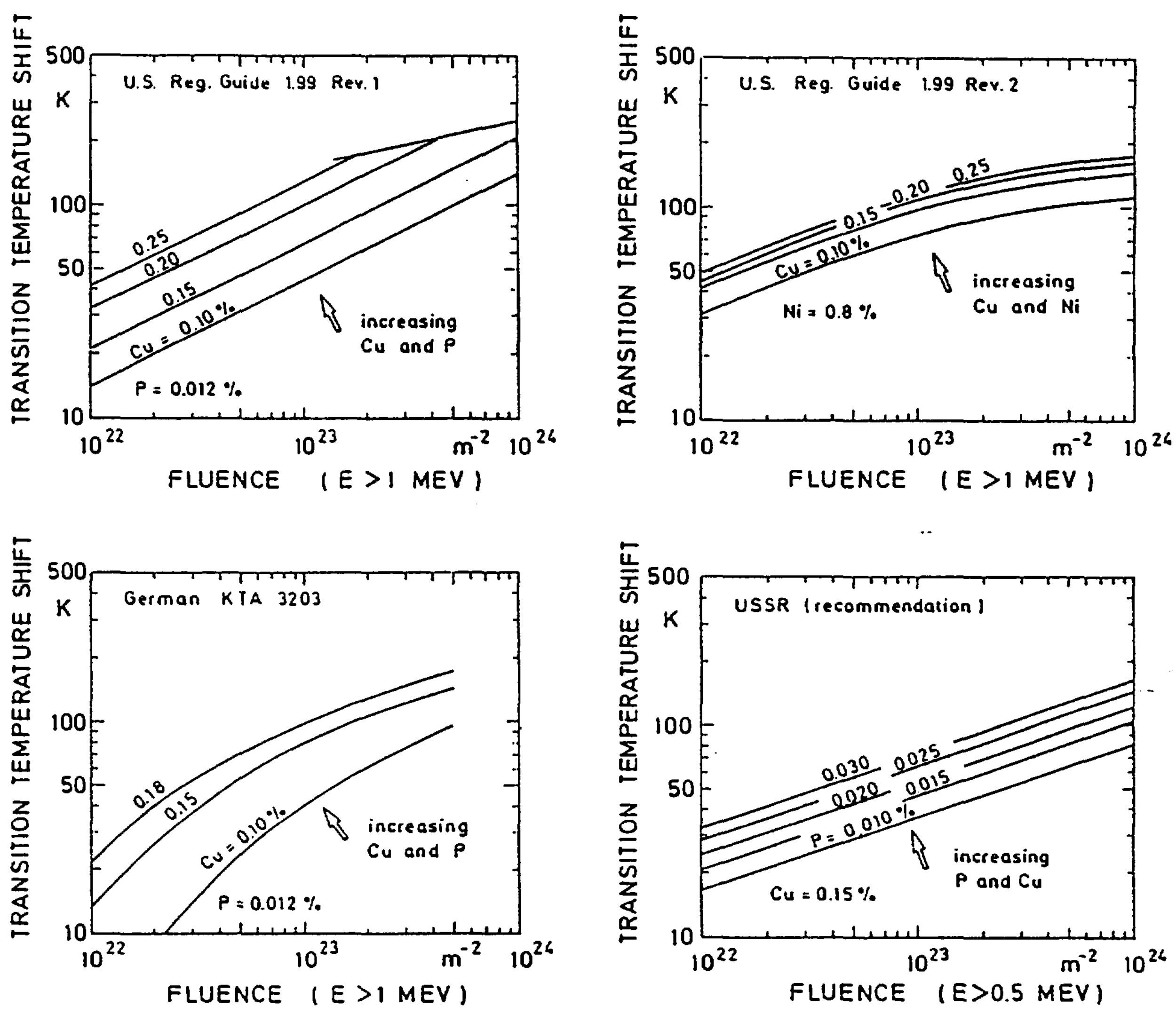
U.S. Reg. Guide 1.99 Rev. 1
TRANSITION TEMPERATURE SHIFT
K
0.25
0.20
0.15
Cu = 0.10 %
P = 0.012 %
increasing Cu and P
FLUENCE (E >1 MEV)
U.S. Reg. Guide 1.99 Rev. 2
0.15
0.20
0.25
Cu = 0.10 %
Ni = 0.8 %
increasing Cu and Ni
German KTA 3203
0.18
0.15
Cu = 0.10 %
P = 0.012 %
USSR (recommendation)
0.030
0.025
0.020
0.015
P = 0.010 %
Cu = 0.15 %
increasing P and Cu
FLUENCE (E>0.5 MEV)

FIGURE 14

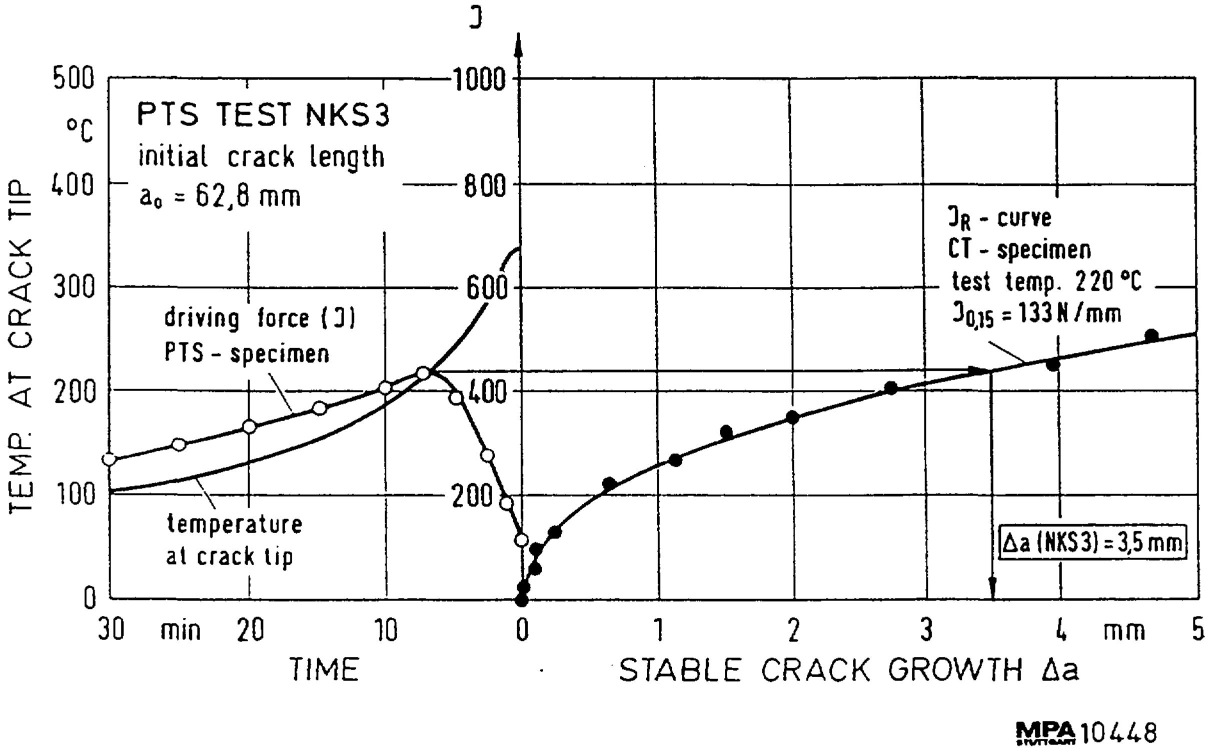
J
PTS TEST NKS3
initial crack length
a_0 = 62,8 mm
TEMP. AT CRACK TIP
°C
500
400
300
200
100
0
1000
800
600
400
200
driving force (J)
PTS - specimen
temperature
at crack tip
J_R - curve
CT - specimen
test temp. 220 °C
$J_{0,15}$ = 133 N/mm
Δa (NKS3) = 3,5 mm
30
min
20
10
0
1
2
3
4
mm
5
TIME
STABLE CRACK GROWTH Δa
MPA 10448

FIGURE 15

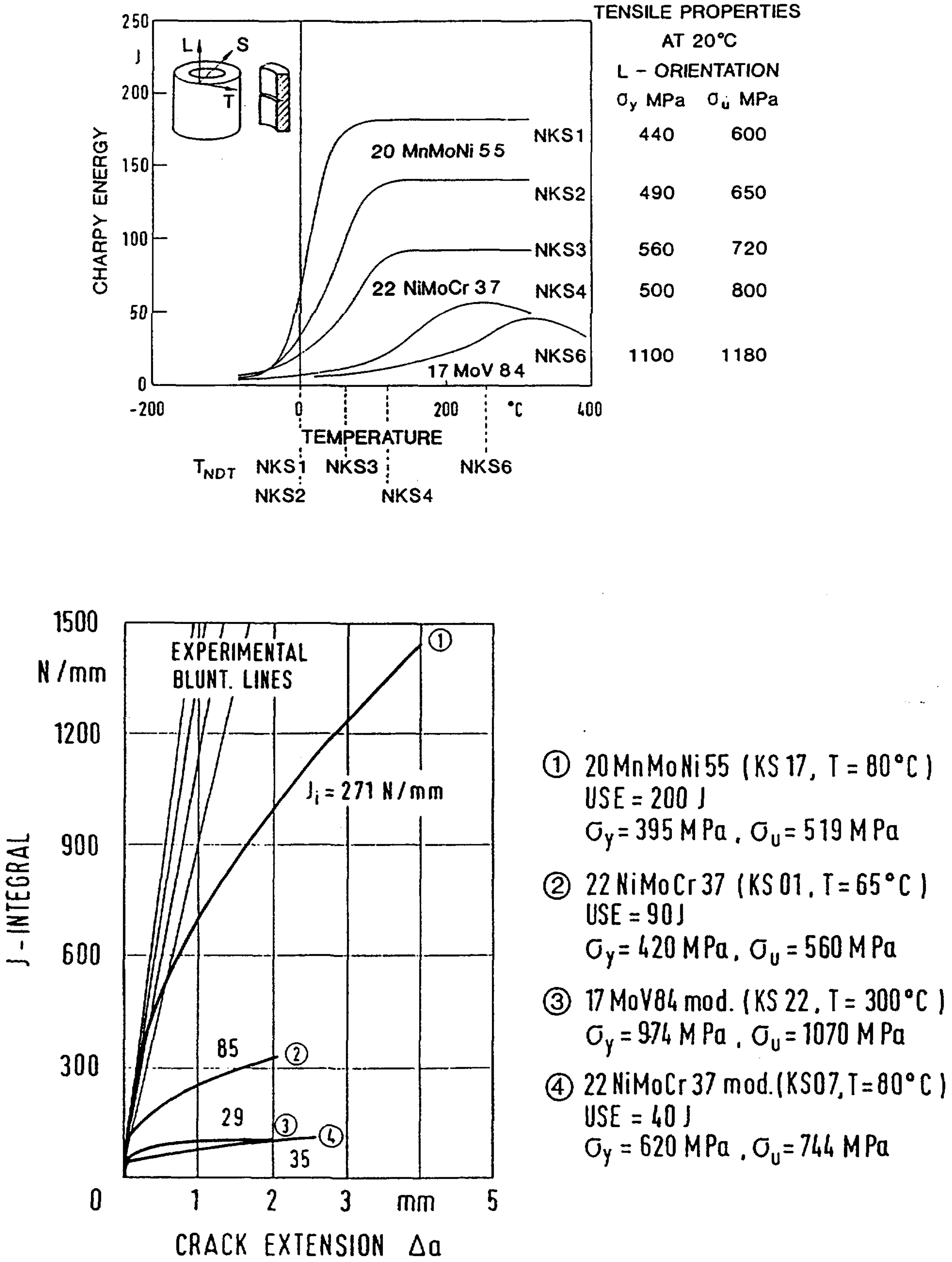

CHARPY ENERGY
J
250
200
150
100
50
0
-200
0
200
°C
400
TEMPERATURE
L
S
T
20 MnMoNi 5 5
22 NiMoCr 3 7
17 MoV 8 4
NKS1
NKS2
NKS3
NKS4
NKS6
T_{NDT} NKS1 NKS3 NKS6
NKS2 NKS4
TENSILE PROPERTIES
AT 20°C
L - ORIENTATION
σ_y MPa σ_u MPa
440 600
490 650
560 720
500 800
1100 1180
J-INTEGRAL
1500
N/mm
1200
900
600
300
0
1
2
3
mm
5
CRACK EXTENSION Δa
EXPERIMENTAL
BLUNT. LINES
$J_i = 271$ N/mm
85
29
35
① 20MnMoNi55 (KS 17, T = 80°C)
USE = 200 J
$\sigma_y = 395$ MPa, $\sigma_u = 519$ MPa
② 22NiMoCr37 (KS 01, T = 65°C)
USE = 90 J
$\sigma_y = 420$ MPa, $\sigma_u = 560$ MPa
③ 17MoV84 mod. (KS 22, T = 300°C)
$\sigma_y = 974$ MPa, $\sigma_u = 1070$ MPa
④ 22NiMoCr37 mod. (KS07, T=80°C)
USE = 40 J
$\sigma_y = 620$ MPa, $\sigma_u = 744$ MPa

FIGURE 16

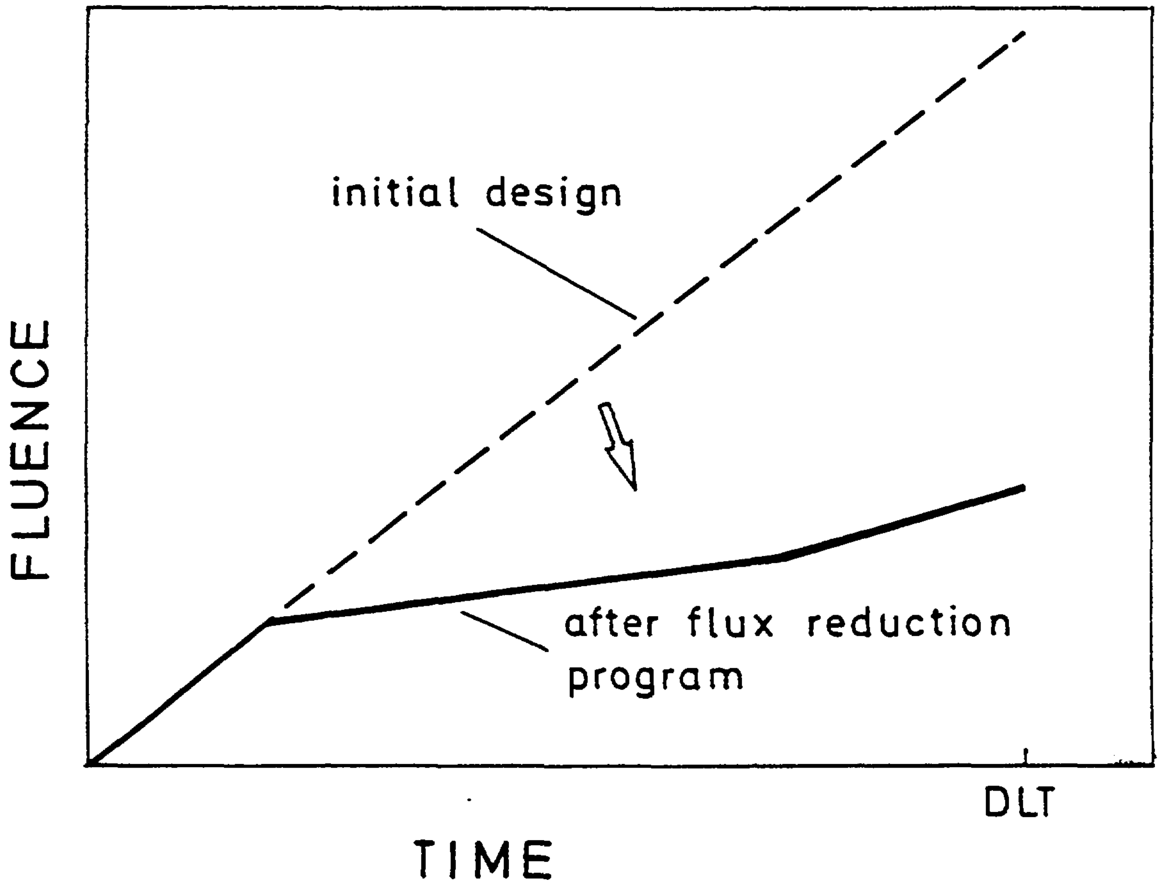
initial design
FLUENCE
after flux reduction program
DLT
TIME

FIGURE 17

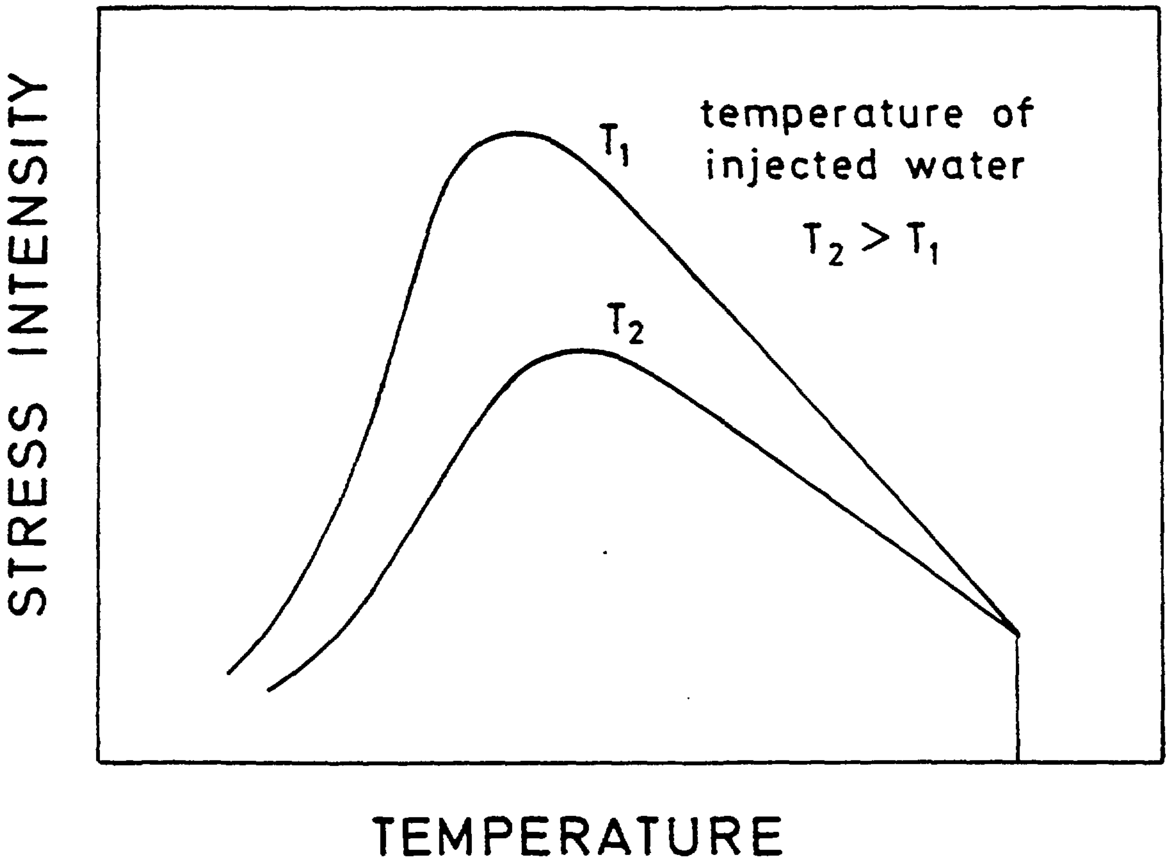
STRESS INTENSITY
temperature of
injected water
$T_2 > T_1$
T_1
T_2
TEMPERATURE

FIGURE 18

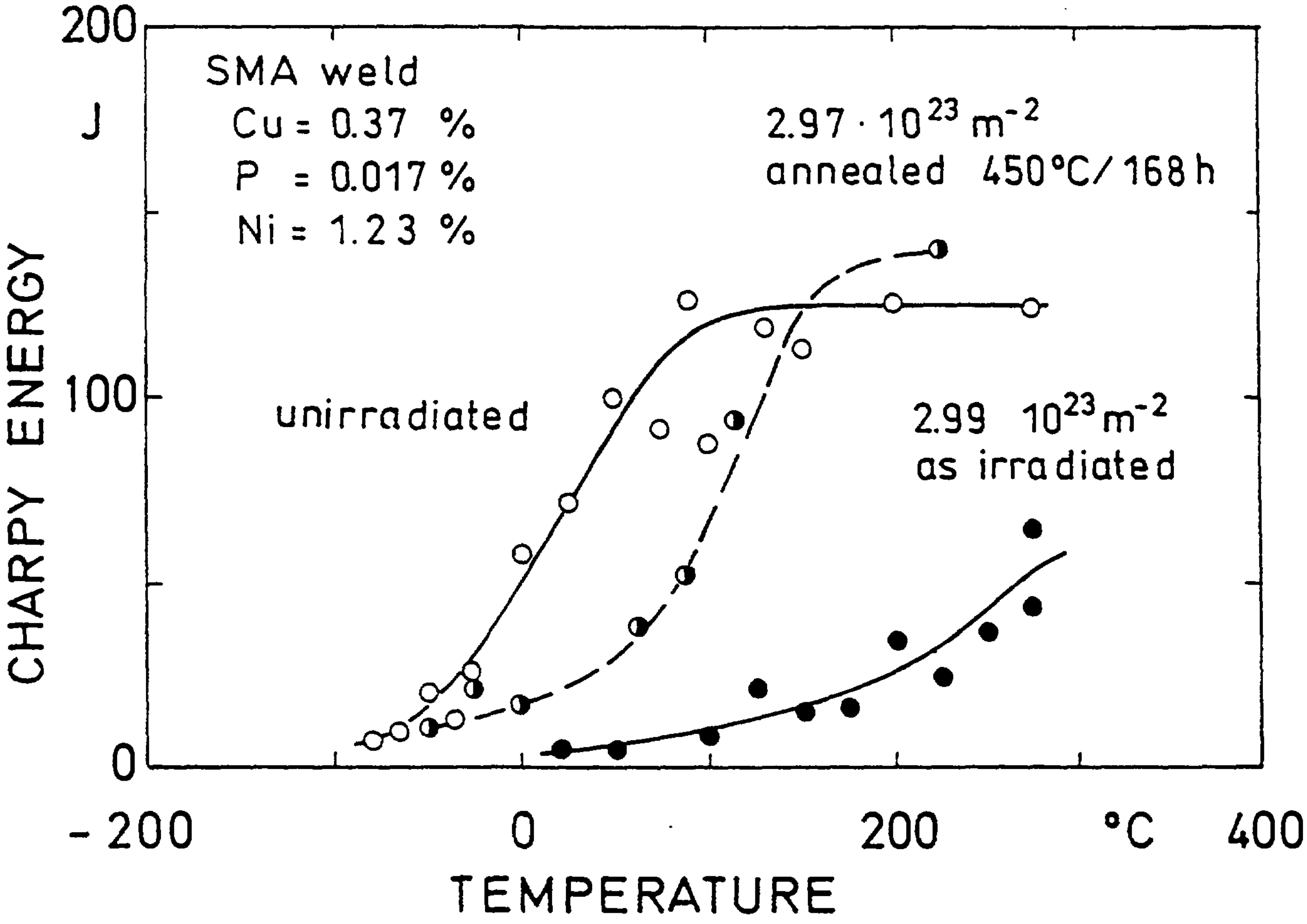
SMA weld
Cu = 0.37 %
P = 0.017 %
Ni = 1.23 %
$2.97 \cdot 10^{23}$ m^{-2}
annealed 450°C/168 h
unirradiated
$2.99\ 10^{23}$ m^{-2}
as irradiated
CHARPY ENERGY
J
200
100
0
-200
0
200
°C
400
TEMPERATURE

FIGURE 19

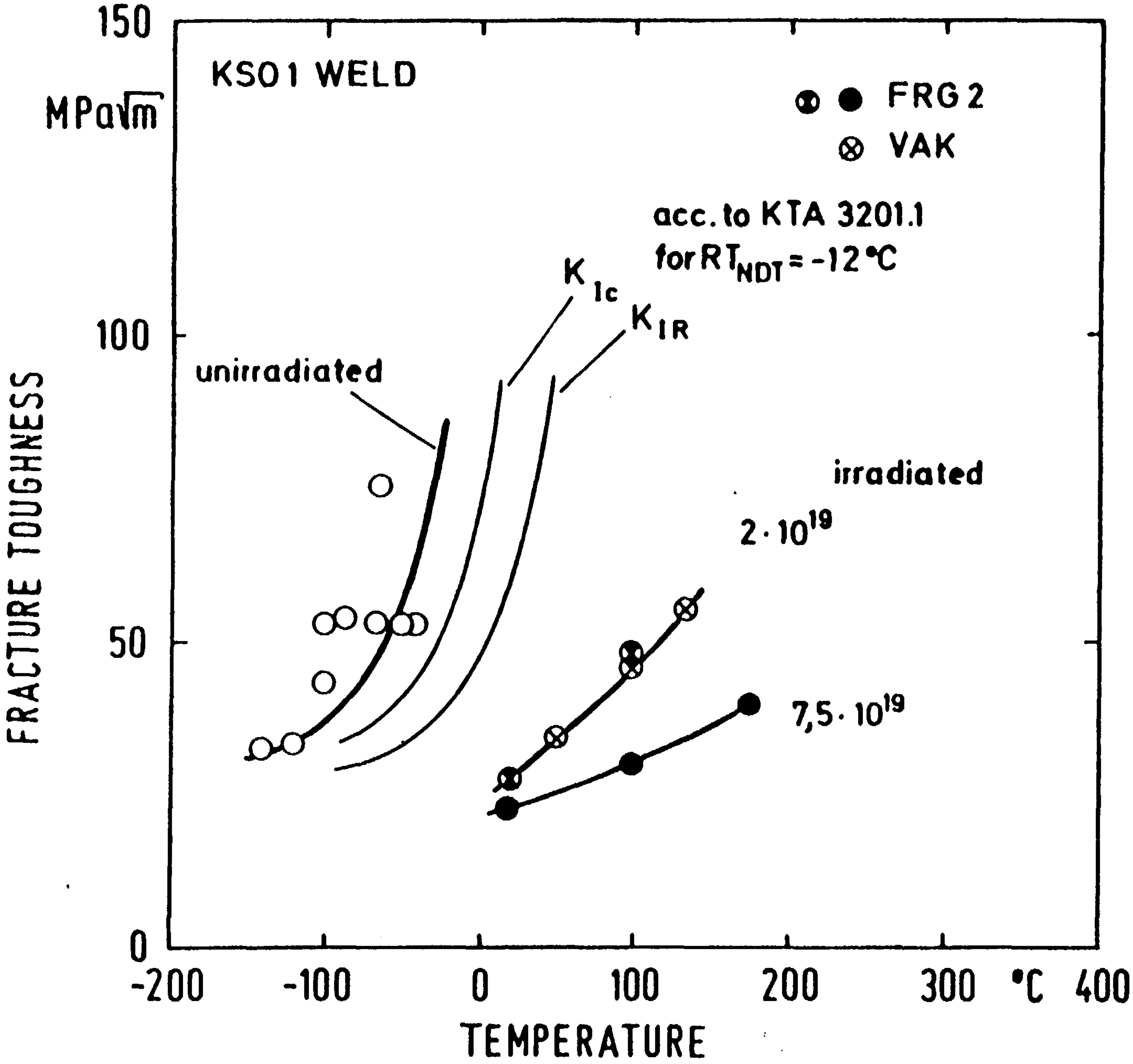

Φ cm^{-2}	σ_y MPa	σ_u MPa
$2{,}0 \cdot 10^{19}$	890	935
$4{,}33 \cdot 10^{19}$	925	965

FIGURE 20

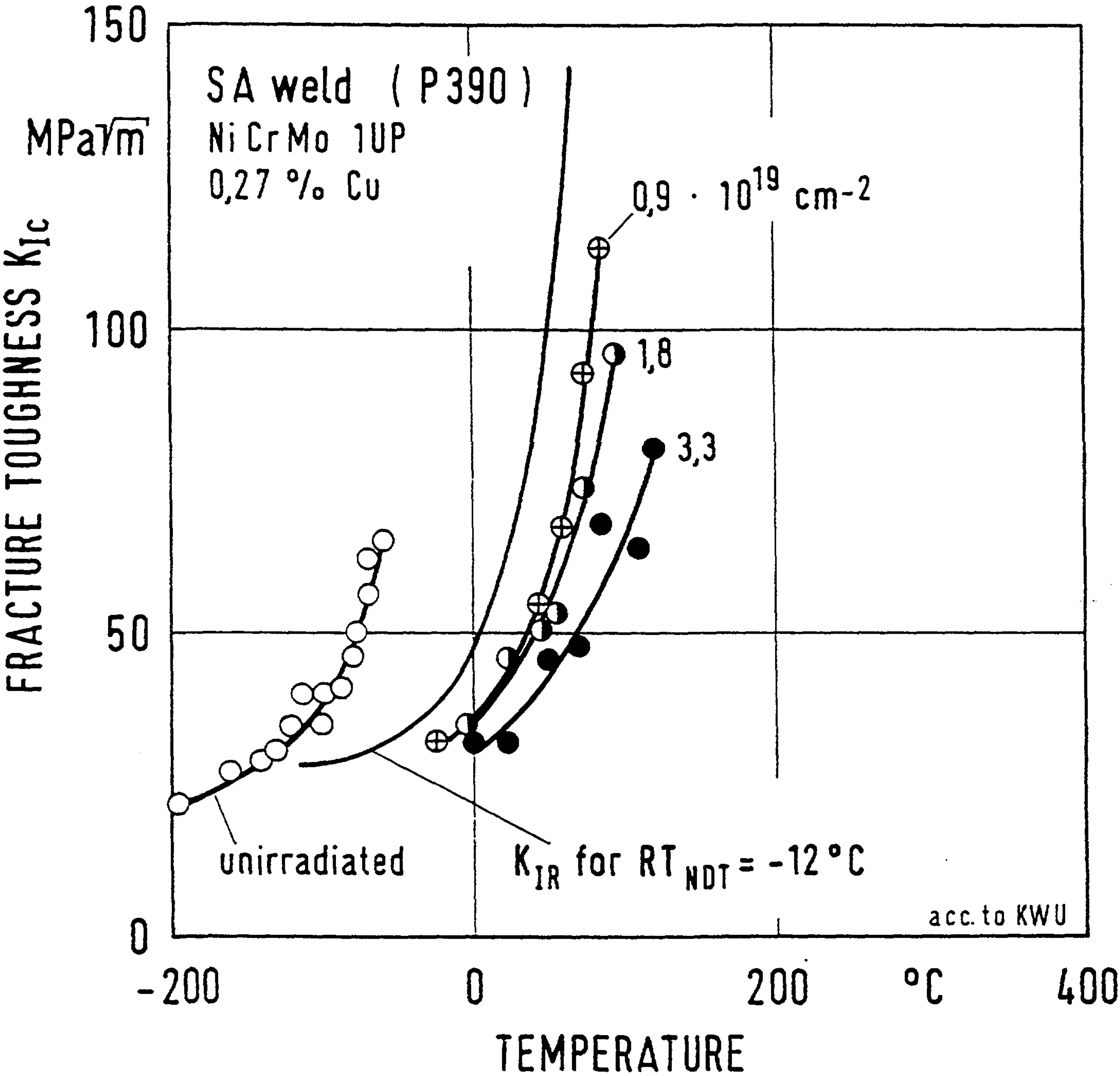

MPA STUTTGART 10452

FIGURE 21

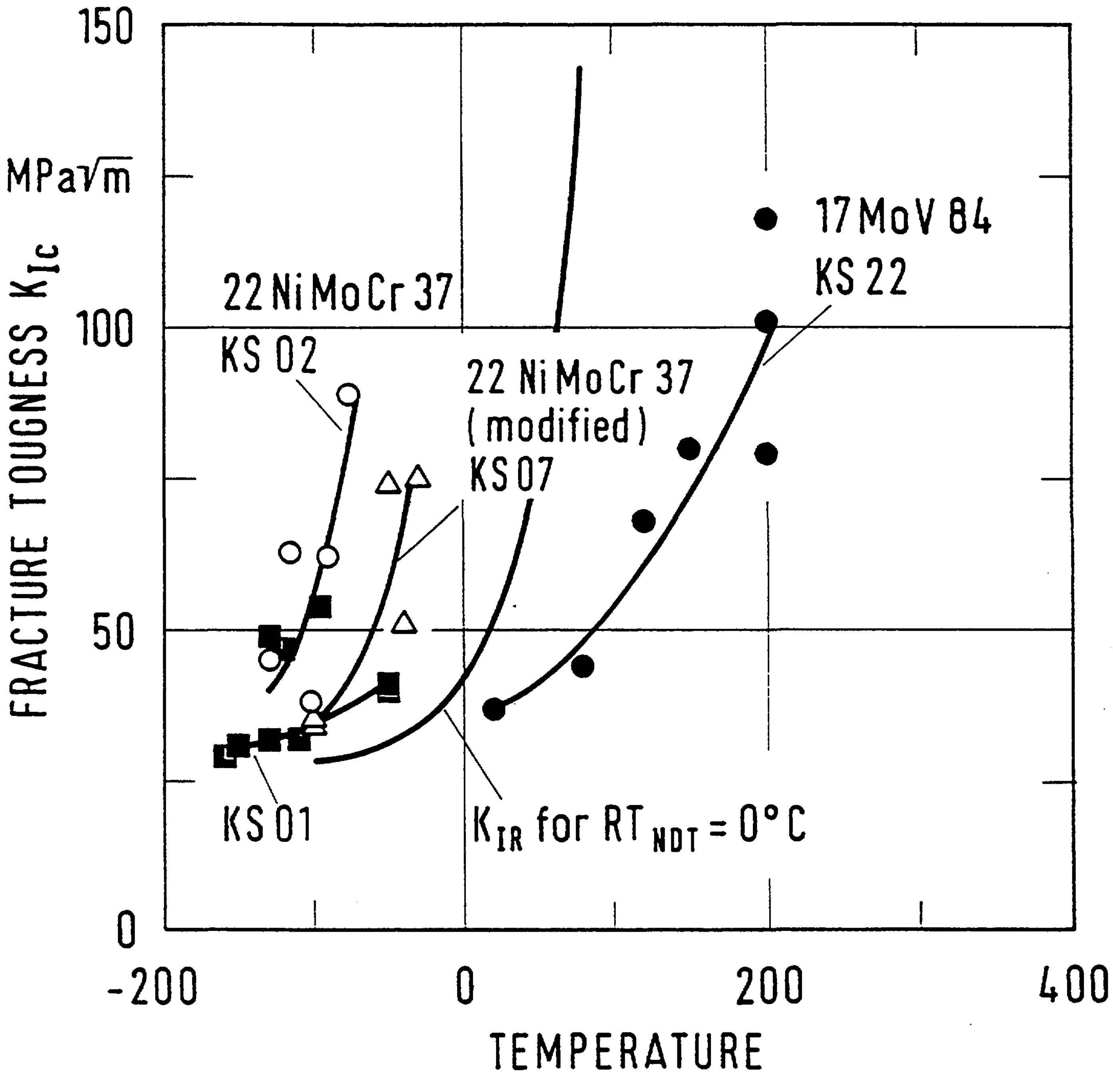
150
MPa√m
100
50
0
-200
0
200
400
FRACTURE TOUGNESS K_{Ic}
TEMPERATURE
17 MoV 84
KS 22
22 NiMoCr 37
KS 02
22 NiMoCr 37
(modified)
KS 07
KS 01
K_{IR} for RT_{NDT} = 0°C

FIGURE 22